FABRICATION AND TESTING OF SMALL SCALE METALLIC CENTRIFUGAL AIR COMPRESSOR

Muhammad Sameer
F2020206013

Mohammad Bilal Hussain
F2020206017

Rafey Ahmad Khakwani
F2020206021

Mohammad Mohyuddin
F2020206037

BSc Aircraft Maintenance Engineering Technology,

Supervised by: Prof. Dr. Ahmad Aizaz

2024

University Of Management & Technology, Lahore

Fabrication and Testing of Small Scale Metallic Centrifugal Air Compressor

Muhammad Sameer
F2020206013

Mohammad Bilal Hussain
F2020206017

Rafey Ahmad Khakwani
F2020206021

Mohammad Mohy Ud Din
F2020206037

Submitted in the partial fulfillment of the requirements for the Degree of Bachelors of Aircraft Maintenance Engineering Technology, University of Management and Technology, Lahore.

Supervised by: Prof Dr Ahmad Aizaz

2024

University Of Management & Technology, Lahore

DECLARATION

We, Students of Bachelors of Aircraft Maintenance Engineering Technology in the subject of Aircraft Maintenance Engineering Technology; Session 2020 - 2024, hereby declare that the matter printed in the thesis title Fabrication and Testing of Small Scale Metallic Centrifugal Air Compressor is our own work and has not been printed, published and submitted as research work dissertation or publication in any form in any university, research institution etc. in Pakistan or abroad.

Dated: July 23, 2024

Signature of Deponents

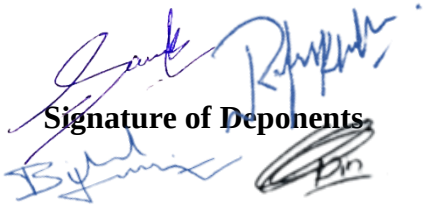

PLAGIARISM UNDERTAKING

We solemnly declare that research work presented in the dissertation titled "**Fabrication and Testing of Small Scale Metallic Centrifugal Air Compressor**" is solely our research work with no significant contribution from any other person. Small contribution or help wherever taken has been duly acknowledged and the complete dissertation has been written by us.

We understand the zero tolerance policy of the HEC and University of Management & Technology towards plagiarism. Therefore, We as Authors of the above titled dissertation declare that no portion of our dissertation has been plagiarized and any material used as references properly referred or cited.

We undertake that if we are found guilty of any formal plagiarism in the above titled dissertation even after award of Bachelor's degree, the University reserves the rights to withdraw or revoke our Bachelor's degree and that HEC and the University has the right to publish our name on the HEC/ University Website on which names of students are placed who submitted plagiarized dissertation.

Muhammad Sameer
Mohammad Bilal Hussain
Rafey Ahmad Khakwani
Mohammad Mohy Ud Din

Dated: July 23, 2024

SIMILARITY REPORT

University of Management and Technology, Lahore

Similarity Report

Turnitin Originality Report
Fabrication and Testing of Small Scale Metallic Centrifugal Air Compressor by Muhammad Sameer Sarwar,mohammad Bilal Hussain, Rafey Ahmad Khakwani, Mohammad Mohy Ud Din

From Quick Submit (Quick Submit)

- Processed on 02-Jul-2024 15:22 PKT
- ID: 2411594345
- Word Count: 5077

Similarity Index

1%

Similarity by Source

Internet Sources:

1%

Publications:

0%

Student Papers:

0%

Sources:

1. 1% match ()
   Prodduturu, Harika Reddy. "Correlation between Roadside Safety Hardware and Vehicle Safety Standards Evaluation Criteria", 2016

2. < 1% match (student papers from 01-May-2020)
   Submitted to Florida Institute of Technology on 2020-05-01

Checked by

Verified by CLO

Note:

- Sometimes the overall similarity index may be a smaller than the repository percentages combined. This would be due to overlapping text within the repositories.

CERTIFICATE OF APPROVAL

Accepted by the Faculty of the Institute of Aviation Studies, University of Management and Technology, Lahore in partial fulfillment of the requirements for the degree Bachelors of Aircraft Maintenance Engineering Technology.

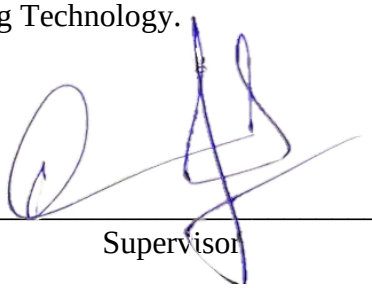

Supervisor

Prof. Dr. Ahmad Aizaz
Institute of Aviation Studies, UMT

External Examiner.

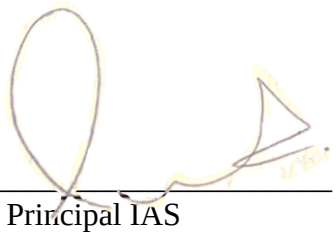

Principal IAS

Capt. Imran Saeed
Institute of Aviation Studies, UMT

Deponents
Muhammad Sameer
Mohammad Bilal Hussain
Rafey Ahmad Khakwani
Mohammad Mohy Ud Din
Institute of Aviation Studies, UMT
Date: July 23, 2024

CERTIFICATE BY SUPERVISOR

I certify that I have read “Fabrication and Testing of Small Scale Metallic Centrifugal Air Compressor” by Muhammad Sameer, Mohammad Bilal Hussain, Mohammad Mohy Ud Din & Rafey Ahmad Khakwani, and that in my opinion this work meets the criteria for approving a dissertation submitted in partial fulfillment of the requirements for the Bachelors of Aircraft Maintenance Engineering Technology at the University of Management and Technology.

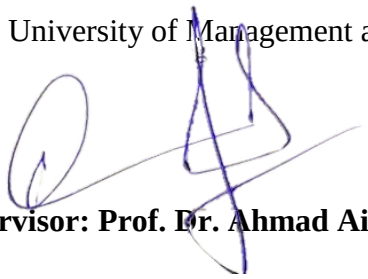

Supervisor: Prof. Dr. Ahmad Aizaz

ABSTRACT

This project's primary objective is the fabrication and testing of small metallic centrifugal air compressor made out of metal alloy, built-in a micro jet engine using MW 54 Turbo Jet Engine as an inspiration which numerous researchers use as basis of development. Centrifugal impeller, an essential element, was made out of high strength Aluminum 2024 –T4 on a 5-axis milling machine; while the structure used 3D printed PLA, PET-G & ABS as part of this hybrid approach in compressor unit design to allow users to see its performance at different speeds. This thesis represents a final phase of work on a project designed to measure pressure & temperature variations between intake impeller components in a controlled environment. Utilizing sets of sensors and controllers to collect systematic data enabling the creation of comprehensive graphs, providing invaluable insights into performance trends. A DC single-shaft motor replacing traditional combustion chamber in this project. Redesigned intake impellers increased airflow within the chamber and are combined with an adjustable variable nozzle that enables unrestricted rotation of the turbine wheel. A small-scale generator measuring the useful power generated from free rotating turbine wheel. All sensors are positioned within the micro jet engine, which is securely mounted on a test stand. This test stand is equipped with four linear bearings to facilitate force measurements. This thesis includes a complete guide on designing, manufacturing, assembly, electronic wiring and testing of a micro jet engine centrifugal air compressor.

Keywords: high-strength, 3D printed, manufacturing, assembly, centrifugal air compressor, testing

DEDICATION

We dedicate this research work to the cherished memory of our beloved ones who have passed away, whose love and inspiration continue to guide us. To our parents, whose unwavering support and encouragement have been the cornerstone of our academic journey, we express our deepest gratitude.

Finally, we extend our heartfelt thanks to all the instructors who have imparted their knowledge and wisdom, helping us to reach this milestone. Your collective contributions have been instrumental in the completion of this degree.

ACKNOWLEDGMENT

Thank you to the Institute of Aviation Studies at University of Management and Technology, where we had this invaluable opportunity to undertake and engage in this research project.

Dr. Ahmad Aizaz deserves our sincerest appreciation as our supervisor on this project, for providing invaluable assistance in understanding its concepts and objectives along with his motivational support. We owe him so much!

Further, we extend our appreciation to ***all faculty*** whose expertise was instrumental in aiding us with understanding 3D printing and fabrication concepts - which ultimately contributed to the successful execution of our project.

Muhammad Sameer
Mohammad Bilal Hussain
Mohammad Mohy Ud Din
Rafey Ahmad Khakwani
Institute of Aviation Studies, UMT
University of Management and Technology, Lahore.

TABLE OF CONTENTS

DECLARATION ii
PLAGIARISM UNDERTAKING iii
SIMILARITY REPORT iv
CERTIFICATE OF APPROVAL v
CERTIFICATE BY SUPERVISOR vi
ABSTRACT vii
DEDICATION viii
ACKNOWLEDGMENT ix
GLOSSARY xii
NOMENCLATURE OR NOTATION xii
LIST OF FIGURES AND TABLES xiii
Chapter 1 1
Introduction 1
Background 2
Aims 3
Objectives 3
Chapter 2 4
History 4
Literature Review 6
Chapter 3 8
Methodology 8
Chapter 4 16
Fabrication 16
3D Printing 16
Test Stand 19
Data Acquisition Box & Board 21
Impeller Fabrication 22
Acrylic Chamber Molding 23
Chapter 5 24
Electrical Circuitry 24
Sensors & Components 24

Block Diagram 25
Schematic Diagram 26
Pin Configurations.....27
Wiring.....28
Programming 29
Micro-controller (Arduino Mega) 29
Wi-Fi Module (ESP 32) 29
Web Portal Development 30
Chapter 6.....32
Assembly 32
Chapter 7.....35
Testing 35
Normal Condition.....35
Stall Condition.....41
Surge Condition.....44
Analysis 47
Standard Condition.....47
Stall Condition.....47
Surge Condition.....48
Sources of Errors.....48
Chapter 8.....49
Conclusion.....49
Future Improvements 49
References.....50
APPENDICES 51
Appendix A.....51
Appendix B.....52

GLOSSARY

Mach number (M)

Speed of Flow (V)

Speed of Sound (a)

NOMENCLATURE OR NOTATION

NGV	Nozzle guide vanes
IGV	Inlet guide vanes
BMP	Barometric Pressure
RPM	Revolutions per Minute
Pc	Chamber Pressure
Tc	Chamber Temperature
Pe	Exhaust Pressure
Te	Exhaust Temperature
Tm	Motor Temperature
CPR	Compression Pressure Ratio
CTR	Compression Temperature Ratio

LIST OF FIGURES AND TABLES

Figure 1.1 Components of Centrifugal Compressor……..……...… 1
Figure 2.1 Whittle W.1X Engine……..... 4
Figure 2.2 MW54 Gas Turbine Engine……... 6
Figure 3.1 Design by Wren Turbines……... 8
Figure 3.2 Explode View of the Proposed Micro Jet Assembly…….. 9
Figure 3.3 Proposed Generator Motor Assembly……. 9
Figure 3.4 Proposed Variable Nozzle Assembly…… 10
Figure 3.5 Proposed Motor Holder Assembly…… 11
Figure 3.6 Proposed RPM Deflector…….. 11
Figure 3.7 Proposed Inlet & Compressor Impeller……. 12
Figure 3.8 Autodesk Inventor Software for fitting and alignment…….. 13
Figure 3.9 Proposed Finalized Design of the Micro Jet Engine…….. 13
Figure 3.10 Proposed Test stand for the Micro Jet Engine……. 14
Figure 3.11 Proposed Data Acquisition Box…….. 15
Figure 3.12 Proposed Final Assembly…… 15
Figure 4.1 Ultimaker Software Slicing Process…….. 16
Figure 4.2 Actual 3D Printed Parts……. 18
Figure 4.3 Actual Variable Nozzle Parts…… 18
Figure 4.4 2020 Extrusion cut to size…….. 20
Figure 4.5 Actual Assembly of Test Stand……. 20
Figure 4.6 PVC Sheets Cutting……... 21
Figure 4.7 Drilling for Toggle Switches……. 22
Figure 4.8 Actual Compressor Impeller……. 22
Figure 4.9 Acrylic Sheet Molding…….. 23
Figure 5.1 Block Diagram…….. 25
Figure 5.2 Schematic Diagram……... 26
Figure 5.3 Wiring process…….. 28
Figure 5.4 Sensor Attached to Vero board……..……... 29
Figure 5.5 Web portal Layout……. 30

Figure 6.1 Actual Nozzle Assembly……... 32
Figure 6.2 Actual RPM Sensor & Motor Placement…….. 33
Figure 6.3 Actual K-type and Chamber Temp. Sensor Placement……...…….. 33
Figure 6.4 Actual Chamber Pressure Tube Placement……...…… 33
Figure 6.5 Actual completed Assembly…….. 34
Figure 7.1 Pressure Change vs RPM at Normal Condition……...…….. 36
Figure 7.2 Temperature Change vs RPM at Normal Condition ……...……... 36
Figure 7.3 CPR Change vs RPM at Normal Condition……..…… 37
Figure 7.4 CTR Change vs RPM at Normal Condition……..…… 37
Figure 7.5 Temperature Change vs RPM at Normal Condition ……... 39
Figure 7.6 Power vs RPM at Normal Condition …….……... 39
Figure 7.7 Efficiency vs RPM at Normal Condition ……..…… 40
Figure 7.8 Pressure Change vs Time at Stall Condition ……..…….. 42
Figure 7.9 Temperature Change vs Time at Stall Condition ……...……... 42
Figure 7.10 CPR Change vs Time at Stall Condition ……..…….. 43
Figure 7.11 CTR Change vs Time at Stall Condition ……..…….. 43
Figure 7.12 Pressure Change vs Time at Surge Condition ……..... 45
Figure 7.13 Temperature Change vs Time at Surge Condition ……. 45
Figure 7.14 CPR Change vs Time at Surge Condition …….. 46
Figure 7.15 CTR Change vs Time at Surge Condition …….. 46

Table 4.1 Micro Jet Part Material Selection…….. 17
Table 4.2 Test Stand Parts……. 19
Table 4.3 PVC Boards……... 21
Table 4.4 Transparent Chamber Cylinder……. 23
Table 5.1 Sensor & Components……... 24
Table 5.2 Pin Configurations……. 27
Table 5.3 Graphical Visualization on Web portal……. 31

Table 7.1 Normal Condition Test Readings……..…… 35

Table 7.2 Additional Normal Condition Test Readings…… 38

Table 7.3 Stall Condition Test Readings……...…… 41

Table 7.4 Surge Condition Test Readings……...…….. 44

Chapter 1

Introduction

A centrifugal air compressor is an apparatus which converts mechanical energy to compressed air through harnessing centrifugal force. Simply, this means it works by speeding up air incoming through an impeller and slowing it down through another part known as the diffuser; ultimately this leads to increased pressure being reached within its chambers and an increase in air pressure being experienced within them. These impellers may be powered either by electricity or turbine. (Paulsen, 1994).

Understanding the workings of a centrifugal compressor involves examining its intricate components as depicted in Figure 1.1. The airflow begins its course from the inlet plenum, deflecting through the inlet guide vanes (IGV) before entering the inducer. Within the inducer, the flow undergoes deceleration, adopting radial directions and eventually leaving the impeller in the diffuser. Forces generated by the radial velocity component, in tandem with the blade curvature effect, play a pivotal role in stabilizing the boundary layer on the shroud and suction side of the inducer, crucial for minimizing turbulence in the boundary layer and preventing separation under adverse pressure gradients.

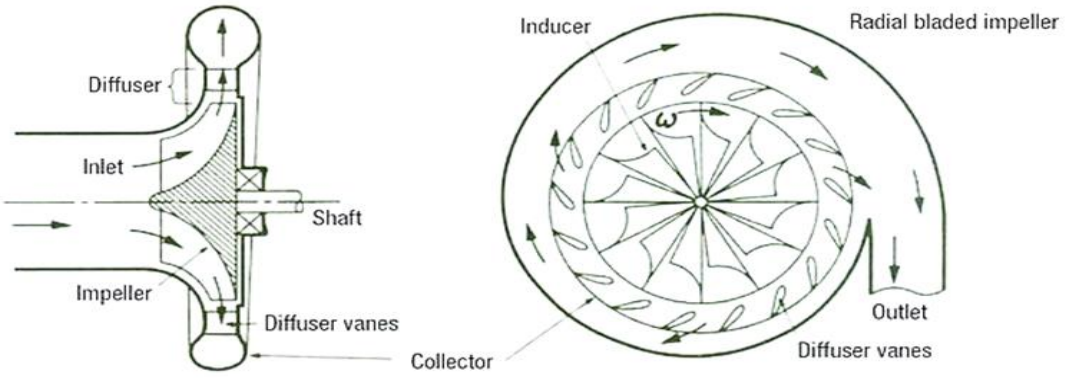

Figure 1.1 Components of Centrifugal Compressor *(Qairblogger, 2017)*

Inner impeller flow patterns feature jet and wake zones with distinct Mach numbers. The jet zone exhibits quasi-isentropic flow, while the wake zone experiences losses from boundary layers and secondary flows. Exiting the impeller, rapid mixing occurs between zones, followed by deceleration due to diffuser radius expansion and wall friction. If Mach number exceeds one, however, shock systems can decelerate flow rendering throat section subsonic. (Braembussche, 2019).

Background

This project, centered on aerospace engineering and manufacturing, involves creating a micro jet engine test stand. Aluminum 2024-T4 was used for the inlet compressor impeller, fabricated on a 5-axis milling system, while other engine components like the diffuser, inlet casings, turbine wheels, and nozzle were 3D printed using PLA, PET-G, and ABS.

Aluminum 2024-T4 was chosen for its excellent strength-to-weight ratio and corrosion resistance, essential for demanding compressor conditions. The 5-axis machine allows precise shaping of the impeller, enhancing performance and efficiency. A transparent acrylic chamber cover provides clear views of internal structures for observation.

Temperature and pressure sensors are incorporated at key locations, generating real-time data. Graphical representation of this data helps understand impeller performance under varying conditions, providing valuable insights.

This project not only focuses on technical manufacturing and material selection but also serves as an educational tool. It offers aerospace and engineering students practical experience with complex systems. By integrating sensors and a data visualization portal, students gain skills in data-driven decision-making, preparing

them for technological challenges in their careers. This innovative educational initiative blends advanced production techniques with hands-on learning, enriching students' understanding of aerospace engineering and fabrication.

Aims

- Development and testing of a functional centrifugal metal air compressor impeller
- Performance evaluation through temperature and pressure measurements
- Introducing innovative design of transparent coverings
- Graphical data visualization

Objectives

- Fabrication and assembly of micro jet engine (excluding combustion chamber)
- Integration with Arduino for data acquisition
- Incorporating 3D-printed structure for innovation
- Development of a functional educational prototype

Chapter 2

History

Micro Jet engines can be broadly defined as engines which utilize the high exiting velocity of jet, gas or liquid jets and convert that energy to forward motion thereby satisfying Newton's third law of motion.

One such early example, known as Aeolipile, utilized heated water (in a circular container) heated using hot air and produced torque as steam left through two of its nozzles to generate forceful thrust against an opponent. However, Dr. Hans von Ohain and Sir Frank Whittle stand out as being two prominent innovators who contributed towards creating modern jet engines we recognize today. Both dedicated themselves towards developing these cutting edge engines which exist today. Sir Frank Whittle registered the schematics of his jet engine first in 1930; Figure 2.1 depicts its successful operation by 1941. Dr. Hans von Ohain followed suit registering his works in 1936 before flying his initial jet engine in 1939 (Bellis, 2019).

Figure 2.1 Whittle W.1X Engine *(NASM, 2022)*

At World War II, engines developed during 1930s were widely employed on fighter aircrafts to offer greater speed as opposed to ordinary propeller engines. By 1950s, developments of jet engine focused on increasing its compression ratio from 10:1 in its early days all the way up to 40:1 (Sudheer, 2023).

There are generally two main types of compressors used in jet engines - an axial compressor and centrifugal compressor, with centrifugal being taken up here as the focus. Sir Frank Whittle first implemented centrifugal compression in his jet engines which is still used today on some small turbojets and turboshaft engines (NASA, 2021).

Literature Review

Researchers of today began developing small jet engine models as part of aviation and academic studies, aiding experimental investigations, furthering knowledge, and helping advance aerospace propulsion technologies.

Figure 2.2 shows Wren Turbines Limited's small scale jet engine known as MW54 that was developed back in 2004 for hobby, academic and research use. There are two variants available - propeller engine model MW54 and gas turbine model MW54 (developed by Mike Murphy and John Wright to power small aircraft at higher speeds with their ability to fit on smaller airframes).

An average MW54 gas turbine engine typically weighs about 0.7-0.8kg with dimensions of 87mm in diameter by 150mm length and features 75 Newton's (16.8lbs.). Garrett T25 46633500-9 compressor along with well profiled turbine wheel for optimal efficiency; there are 47mm long cooling holes installed behind its rear part which also helps regulate exhaust gas temperature (EGT) (GTEBuilders, 2020).

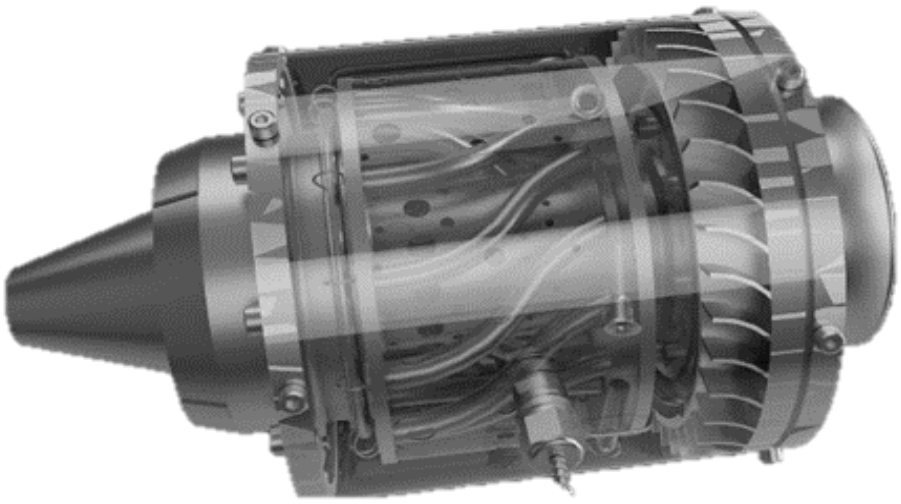

Figure 2.2 MW54 Gas Turbine Engine *(GTEBuilders, 2020)*

Miniature engines have long been utilized in research and academic settings alike, serving both research purposes as well as education purposes. Small scale jet engines have undergone recent advancements that allow them to be installed onto model aircraft, Unmanned Aerial Vehicles (UAVs), and autonomous flight systems. At Technische Universitat Munchen's Institute of Flight Propulsion they are conducting experiments and creating the Frank Turbine TJ 74 with experimental data calculated using GasTurb 12 simulation software for experiments conducted (Hirndorf, 2013).

Chapter 3

Methodology

The methodology was inspired by the MW54 turbojet engine assembly manual, using Autodesk Inventor Software for micro jet engine design. Components like the chamber cover, NGV, turbine wheel, and diffuser were adapted from the MW54 assembly as shown in Figure 3.1. This approach ensured the micro jet engine inherited proven design principles and functionality.

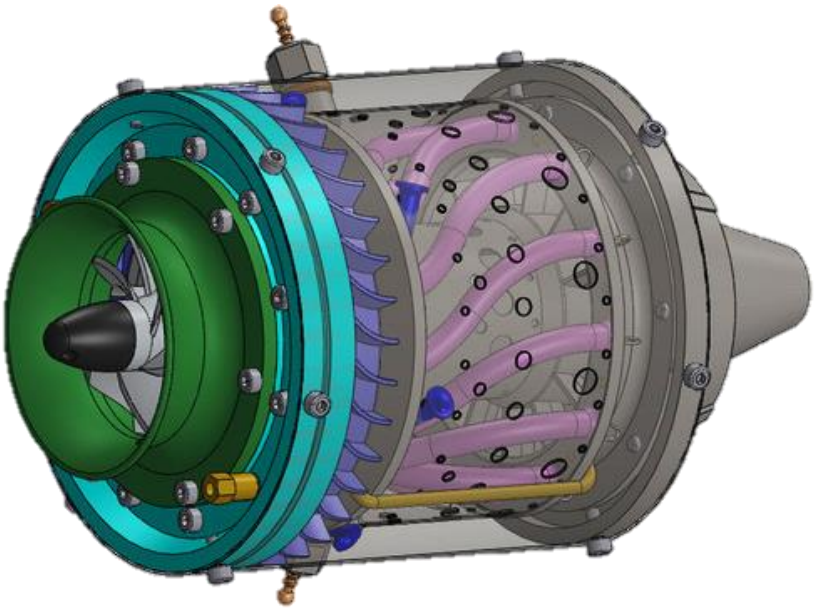

Figure 3.1 Design by Wren Turbines *(Murphy, 2022)*

After utilizing the dimensions and specifications of the MW54 turbojet engine parts from the manual, new components were designed using Autodesk software. These included the compressor impeller, inlet, motor holder, generator motor holder, RPM deflector, DC motor, generator motor, variable nozzle holder, and blades assembly as shown in Figure 3.2. These newly designed parts were integrated into the proposed assembly, ensuring compatibility and functionality within the micro jet engine's design parameters.

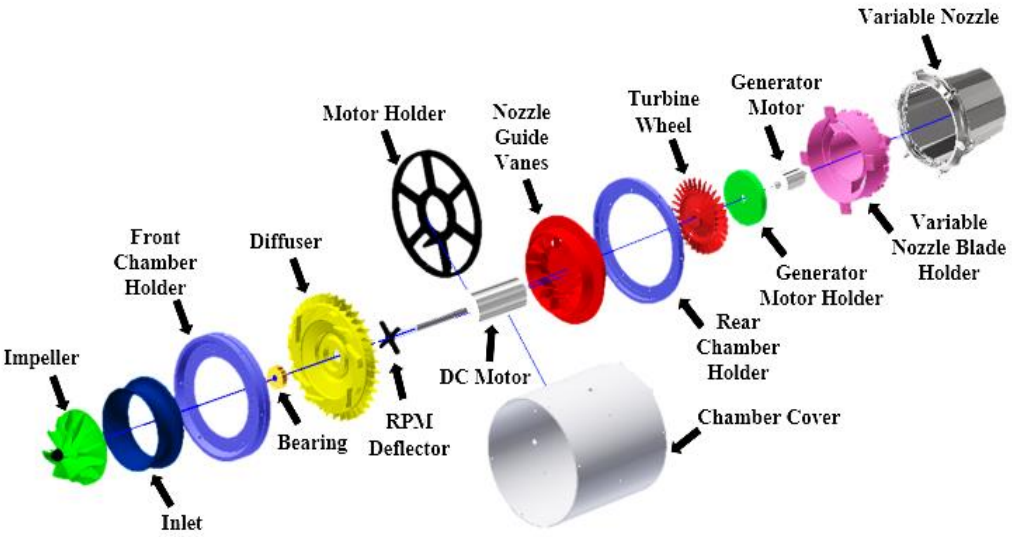

Figure 3.2 Exploded View of the Proposed Micro Jet Assembly

The first component designed was the generator motor holder as shown in Figure 3.3, intended to securely house the generator motor. Positioned after the NGV, which rotate freely in the airflow just before the exit point from the variable nozzle.

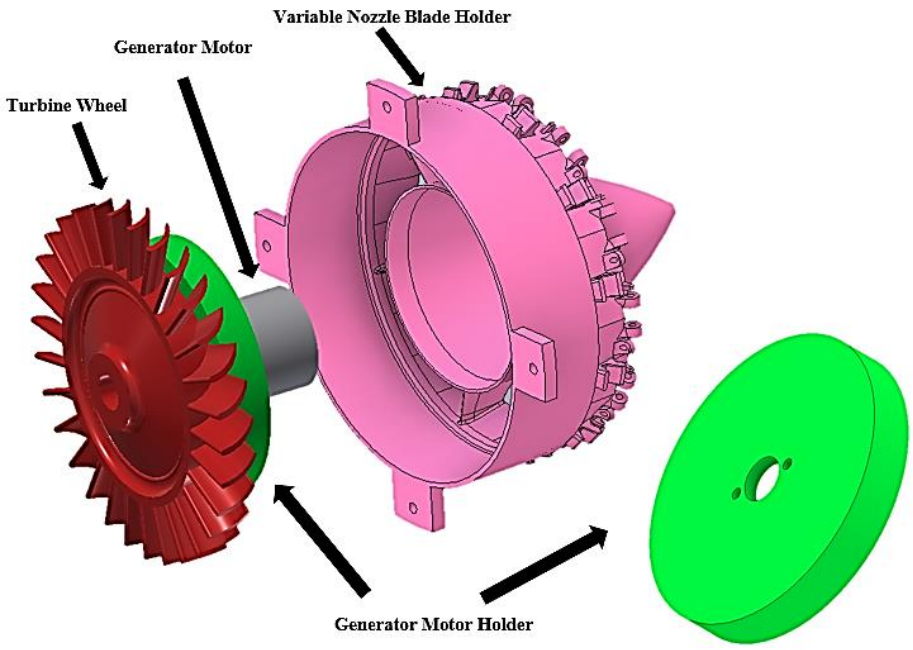

Figure 3.3 Proposed Generator Motor Assembly

The subsequent component designed was the variable nozzle, featuring a ring that secures six control blades and six support blades as shown in Figure 3.4. This

nozzle assembly regulates airflow and thrust direction within the micro jet engine. The ring holds these blades in place on the variable nozzle holder, ensuring control during engine operation.

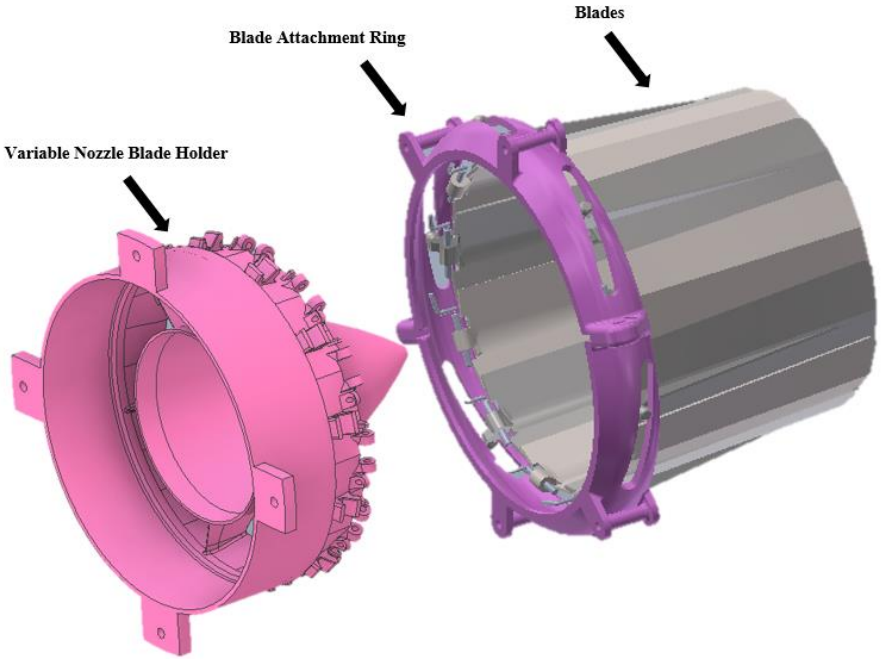

Figure 3.4 Proposed Variable Nozzle Assembly

The motor holder was designed to support the motor, absorb vibrations, and integrate RPM and temperature sensors as shown in Figure 3.5. Bolt points aligned with case holders to secure an acrylic sheet, with a web cage for airflow and cooling efficiency.

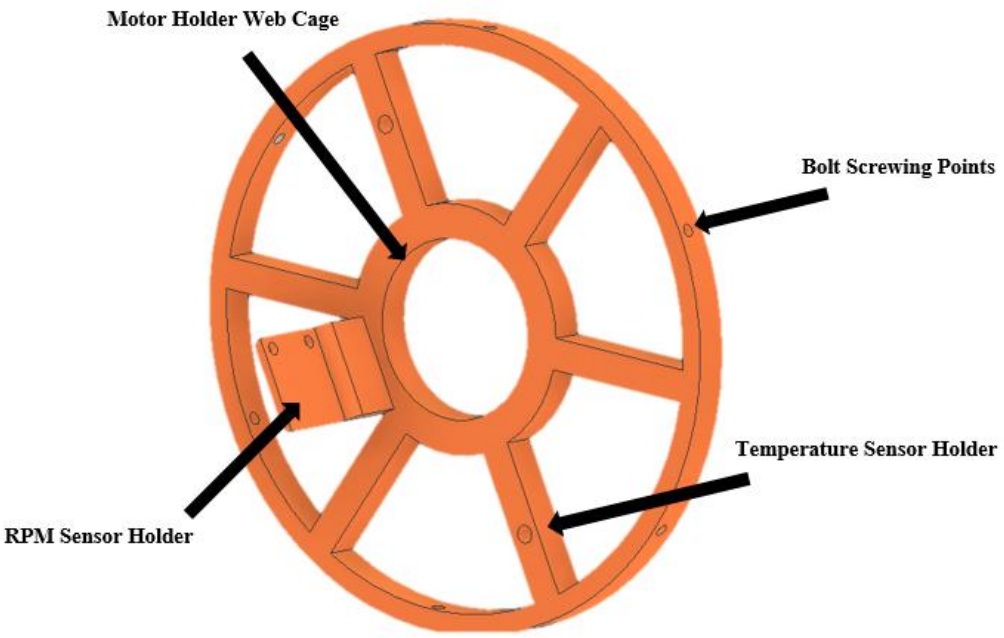

Figure 3.5 Proposed Motor Holder Assembly

The smallest component designed was the RPM sensor deflector, also known as an encoder. This component was crafted to attach to the motor shaft to generate deflections. Its compact size was specifically engineered to enable smooth rotation within the chamber as shown in Figure 3.6, ensuring RPM measurement during operation of the micro jet engine.

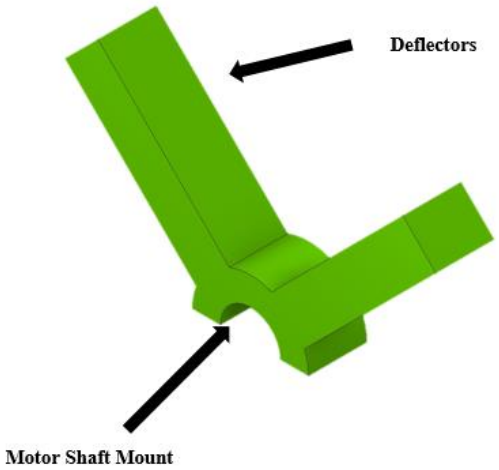

Figure 3.6 Proposed RPM Deflector

The compressor impeller and inlet were designed in Aluminum 2024 T4 for cost-effectiveness and simplicity as shown in Figure 3.7. The design prioritized ease of maintenance and interchangeability of impellers without requiring redesign, enhancing versatility.

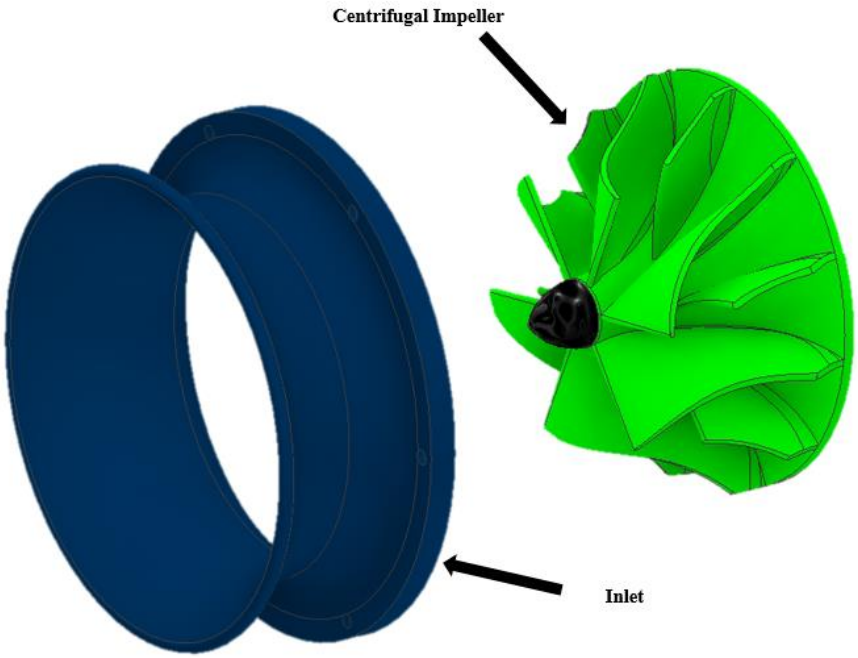

Figure 3.7 Proposed Inlet & Compressor Impeller

Once all parts were fully designed, fitting was performed using Autodesk Inventor software as shown in Figure 3.8 to prevent any potential collisions or tolerance issues during the fabrication process. This fitting process aimed to eliminate the risk of time and budget overruns caused by reworking or replacing parts that do not fit or become damaged due to interferences. By ensuring precise alignment and clearance between components virtually, the design phase aimed to streamline the manufacturing process of the micro jet engine assembly.

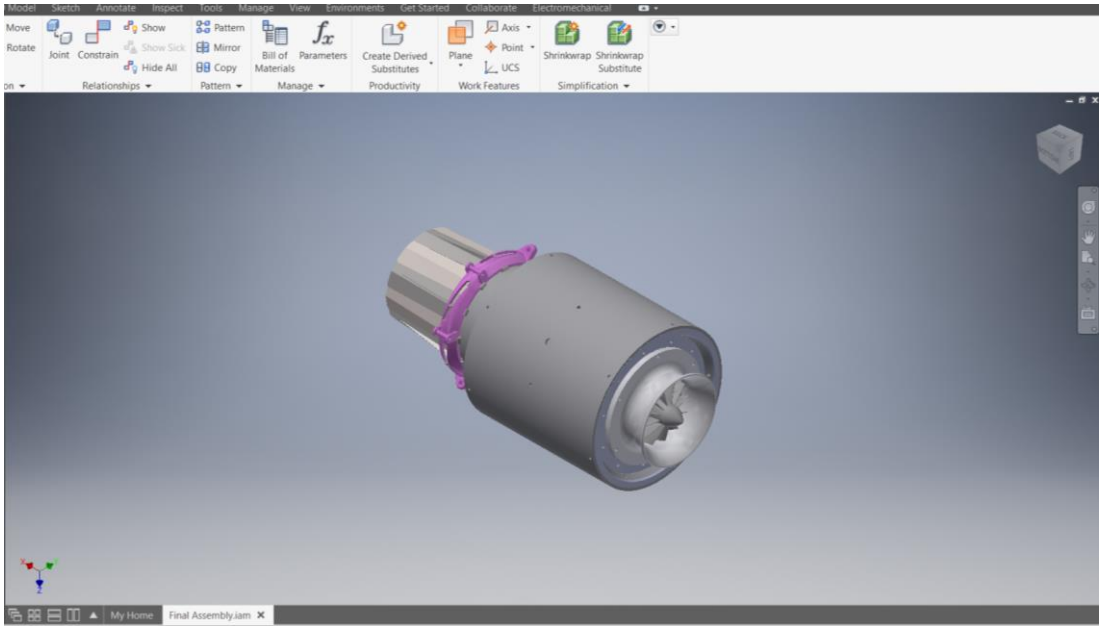

Figure 3.8 Autodesk Inventor Software for fitting and alignment

Software verified tolerances and fittings, followed by confirming structural alignment, dimensions, and aesthetics to finalize adjustments before manufacturing, ensuring design compliance with Figure 3.9, reducing production modifications and optimizing efficiency.

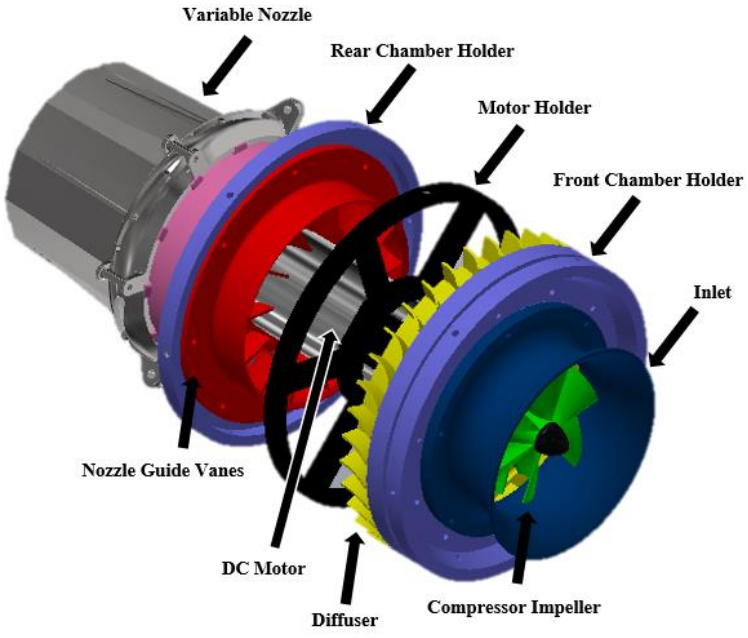

Figure 3.9 Proposed Finalized Design of the Micro Jet Engine

Once the micro jet engine design was finalized in software, a dedicated testing stand was created. It featured a clamping mechanism to secure the engine and a simple structure supported by linear bearings on rods with T holders as shown in Figure 3.10, ensuring ease of engine removal for maintenance and adjustments.

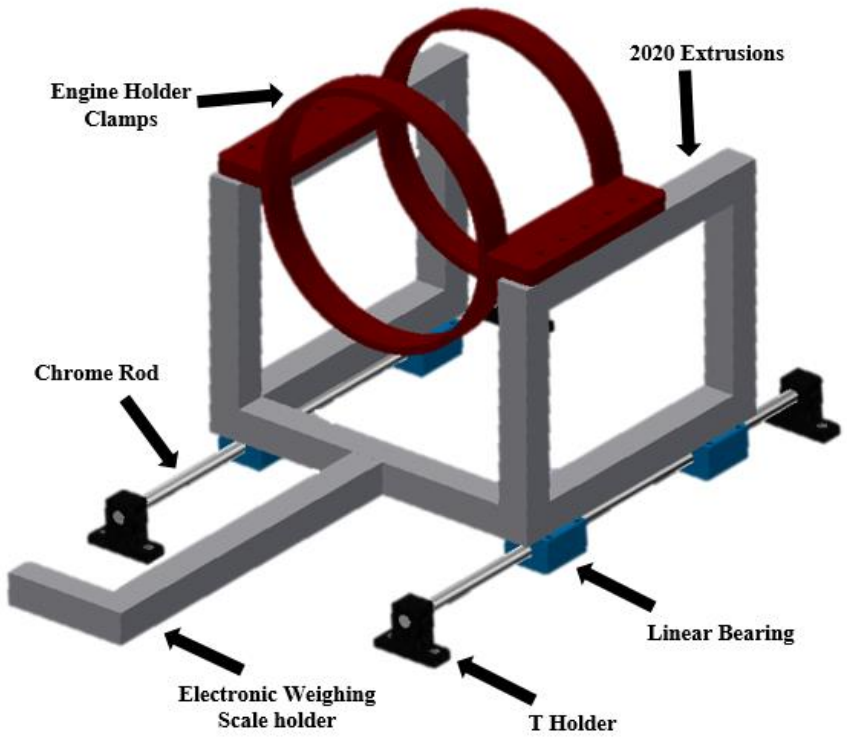

Figure 3.10 Proposed Test stand for the Micro Jet Engine

Towards the final stages of the design phase, a data acquisition box and a supporting board were developed to integrate and organize the entire assembly. The acquisition box was designed with a front interface that accommodated toggle switches and power buttons, providing user-friendly control over the entire setup as shown in Figure 3.11. This configuration ensured convenient access to essential controls and enhanced the operational efficiency of the micro jet engine system.

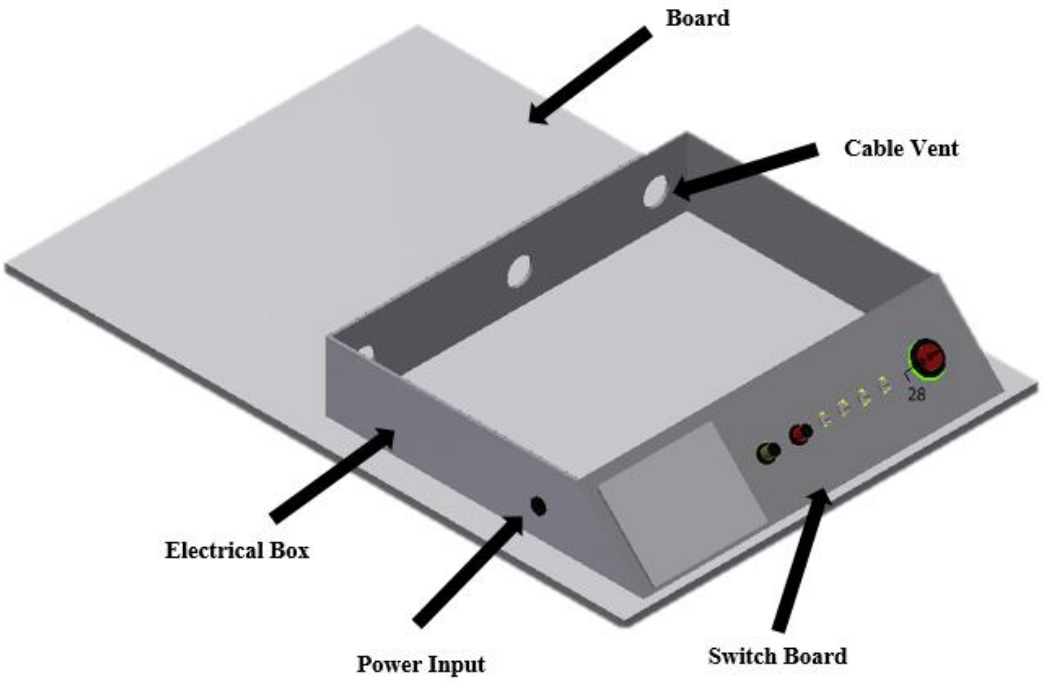

Figure 3.11 Proposed Data Acquisition Box

After an extensive design phase, here is the proposed complete setup of the project shown in Figure 3.12. The next step involves manufacturing each part to bring the design to fruition. All the CAD drawings are mentioned in Appendix B.

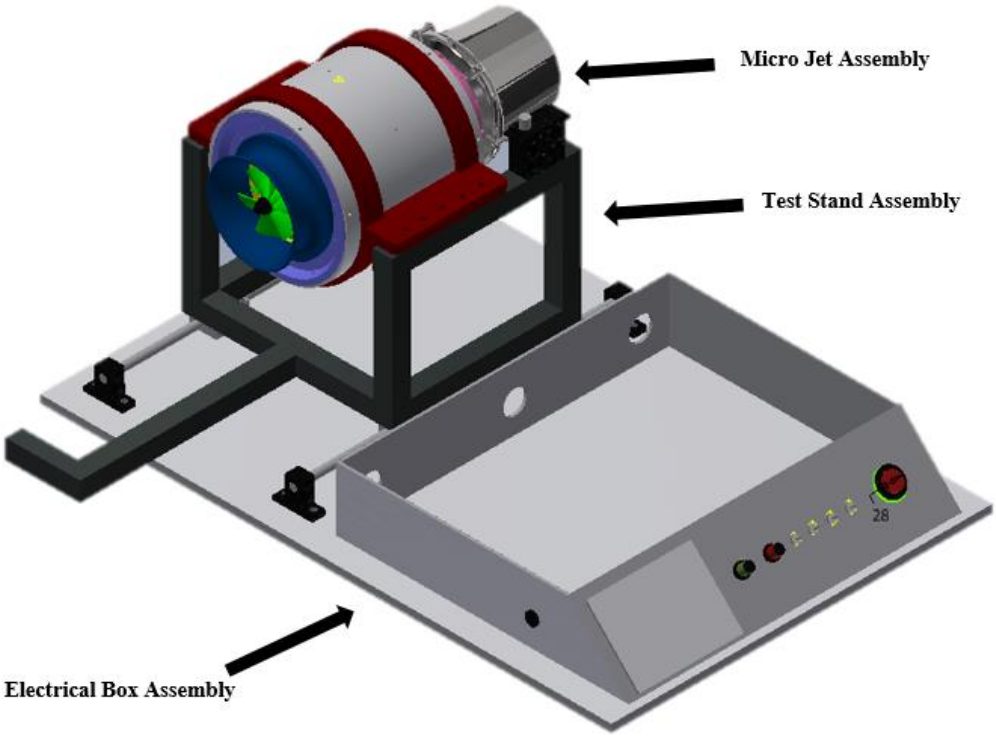

Figure 3.12 Proposed Final Assembly

Chapter 4

Fabrication

The fabrication process started with the 3D printing of the micro jet engine, followed by the test stand, and finally, the data acquisition box and board. The fabrication of the compressor impeller was prioritized last due to its significant cost and the financial constraints limiting the project to a single manufacturing attempt.

3D Printing

The 3D printing process began with the design being entrusted to Buraq Studios, renowned professional 3D printers in Lahore. They reviewed each assembly part, engaging in discussions regarding minor adjustments and tolerance specifications. Prior to printing, all parts underwent slicing using Ultimaker software, followed by initiating the print commands on the 3D printers.

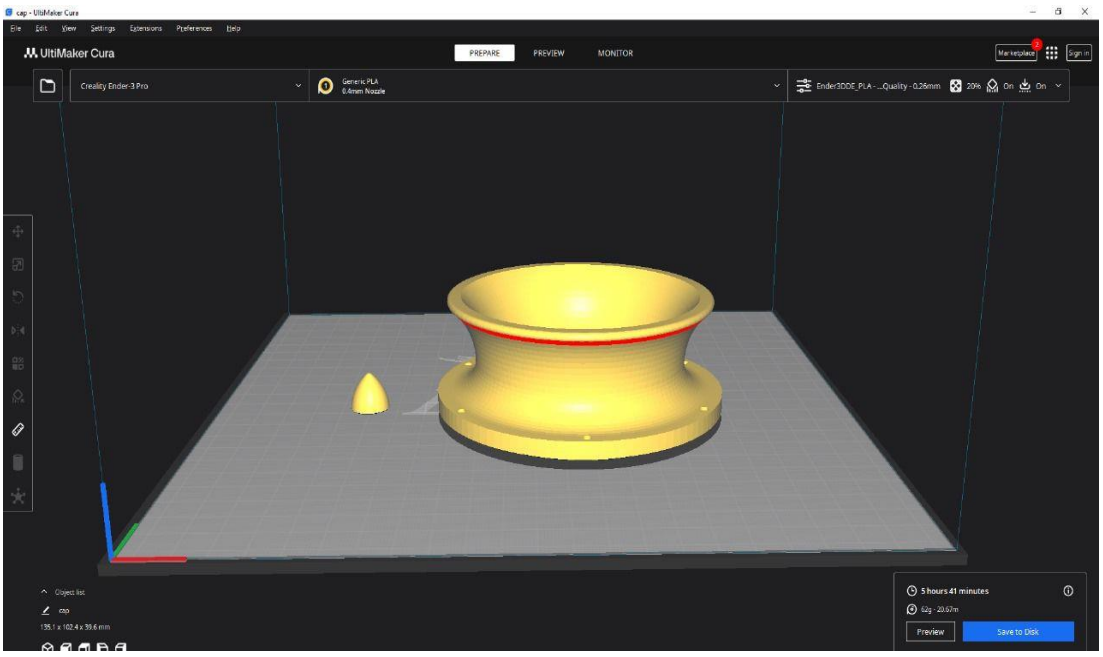

Figure 4.1 Ultimaker Software Slicing Process

The Ultimaker software as shown in Figure 4.1 processed the slicing and calculated the weight of each part, aiding in cost estimation and material selection for the printing process. This step was crucial in determining the feasibility and

optimizing the efficiency of producing each component according to the project's budget and material requirements.

Below, Table 4.1 lists all the structural parts that were 3D printed along with their material selection. Load-bearing parts were printed in PET-G, fast-moving parts were printed in ABS, and small parts that did not require strength were printed in PLA.

Table 4.1

Micro Jet Part Material Selection

Sr #	Part Name	Quantity	Material	Weight	Print Time
1	Inlet	2	PET- G	54 g	6 h
2	Compressor Tip	1	PLA	4 g	30 min
3	Diffuser	1	ABS	135 g	11 h
4	Front Chamber Holder	1	PET-G	72 g	7 h
5	RPM Deflector	2	PLA	15 g	1 h
6	Motor Holder	1	PET-G	55 g	5 h
7	Nozzle Guided Vanes	1	PET - G	102 g	10 h
8	Rear Chamber Holder	1	PLA	66 g	5 h
9	Turbine Wheel	1	ABS	48 g	5 h
10	Generator Holder	1	PET-G	25 g	2 h
11	Nozzle Blade Holder	1	PLA	72 g	6 h
12	Nozzle Ring	1	ABS	16 g	1 h
13	Nozzle Blade	12	ABS	7 g	8 h
14	Engine Clamp	2	PLA	122 g	11 h

It took a total of 80 hours to print all the parts. Figures 4.2 and 4.3 display the various parts that were printed and are now ready for assembly.

Figure 4.2 Actual 3D Printed Parts

Figure 4.3 Actual Variable Nozzle Parts

Test Stand

During the test stand design phase, using 2020 aluminum extrusions facilitated secure engine holding with linear bearing movement. Assembly utilized 90-degree inner joints, T holders, and a chrome rod for smooth bearings (Table 4.2).

Table 4.2

Test Stand Parts

Sr #	**Part Name**	**Quantity**	**Size** (L x W x H)
1	T holder	4	3cm x 1cm x 4cm
2	Chrome Rod	2	35 cm x D 8mm
3	Rectangle	2	20cm x 15cm x 20mm
4	Middle	1	16cm x 20mm x 20mm
5	Weigh Scale Holder	1	22cm x 20mm x 20mm
6	90 inner joint	13	-
7	Linear Bearing	4	4cm x 2.5cm x 2.5cm
8	Bolts	30	M5 - 8

The 2020 extrusions were cut to size using a grinder, and the edges were treated for smoothness and precision, as shown in Figure 4.4. The actual assembly was tightened together using M5-8 bolts and an L key set, as shown in Figure 4.5. This ensured a secure and stable structure for the test stand.

Figure 4.4 2020 Extrusion cut to size

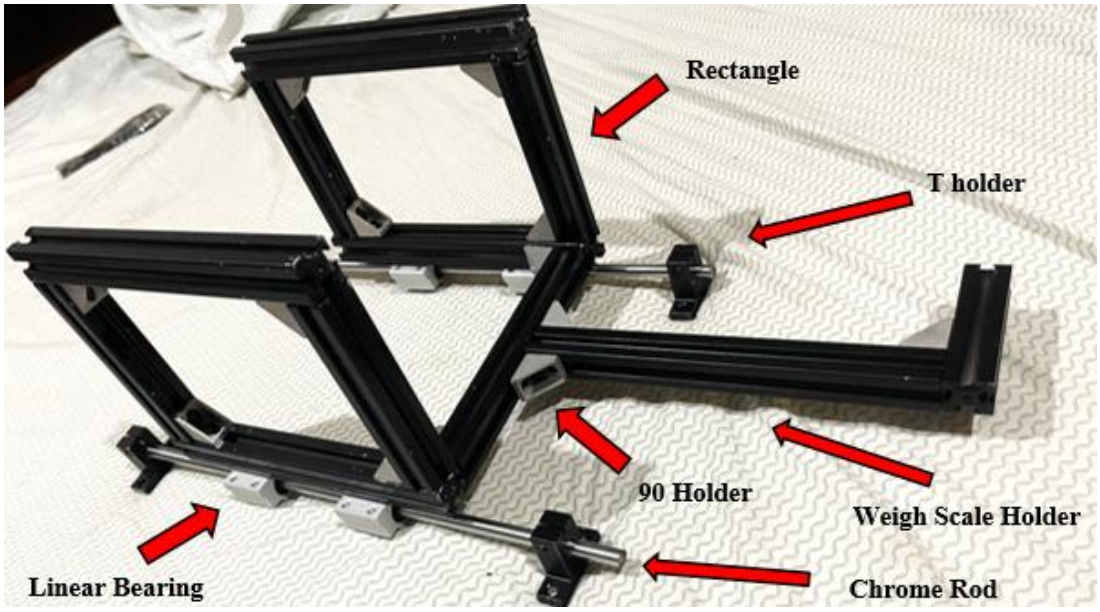

Figure 4.5 Actual Assembly of Test Stand

Data Acquisition Box & Board

The data acquisition box was fabricated in accordance with the design phase specifications. A large board was created to support the entire project, accompanied by a data acquisition box that housed all the sensors and circuitry necessary for the test stand. This setup ensured that all components were organized and securely integrated for efficient testing and operation. All these parts are shown in Table 4.3.

Table 4.3

PVC Boards

Sr #	**Part Name**	**Quantity**	**Size** (L x W x H)
1	Base Board (PVC)	1	38cm x 58cm x 5mm
2	Switch Panel (Front)	1	32 cm x 3mm x 7cm
3	Side Panels L & R	2	29cm x 3mm x 7cm
4	Back Vent Panel	1	32cm x 3mm x 7cm
5	Top Cover Panel	1	32cm x 3mm x 23cm

The PVC boards were cut to the required sizes using a saw machine. The base board was cut from a 5 mm white PVC sheet, while the remaining panels were cut from a transparent 3 mm PVC sheet as shown in Figure 4.6.

Figure 4.6 PVC Sheets Cutting

The front panel was drilled using various drill bits to accommodate the toggle switches and the power switch as shown in Figure 4.7. This ensured that all controls were accessible and securely mounted on the panel.

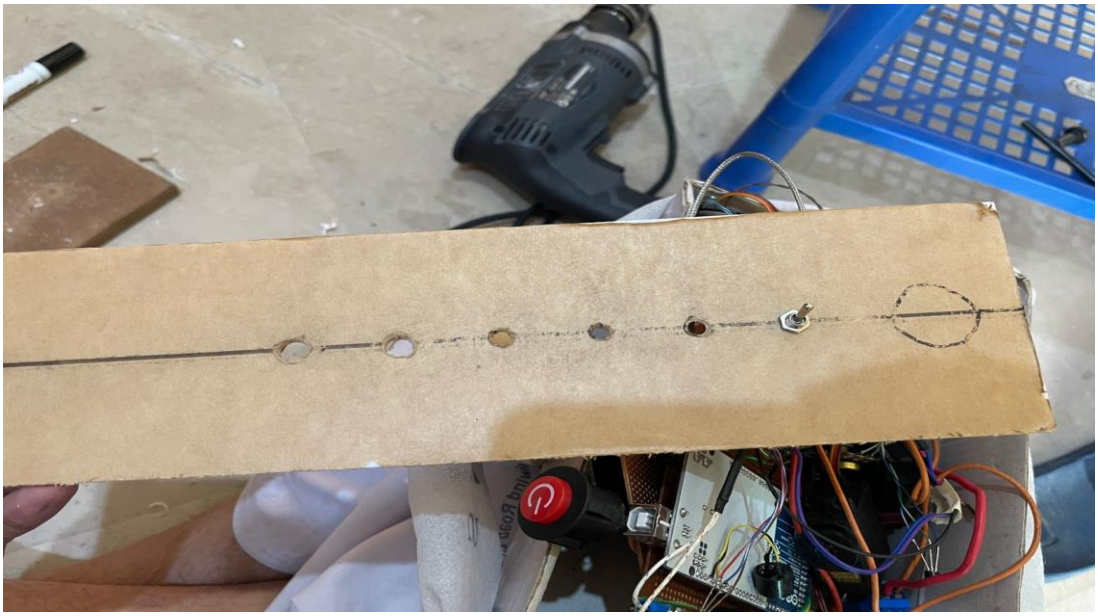

Figure 4.7 Drilling for Toggle Switches

Impeller Fabrication

The centrifugal compressor impeller fabrication process was handled by KIMTECH, a fabrication company located in China. The STL/STP files along with the CAD drawing as shown in Appendix B were sent to them, and they fabricated the

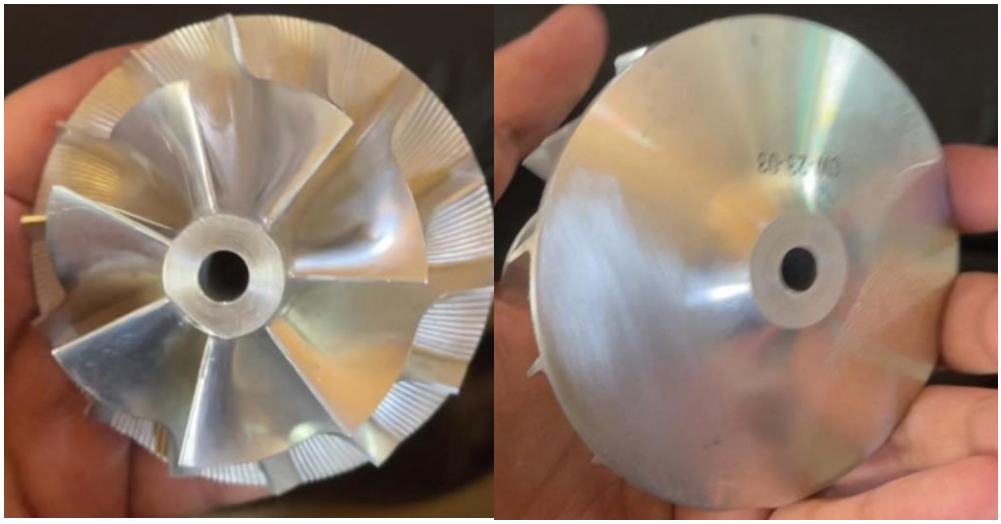

Figure 4.8 Actual Compressor Impeller

impeller using Al 2024-T4 material before shipping it to Pakistan. The Final outcome is shown in Figure 4.8.

Acrylic Chamber Molding

A transparent acrylic chamber was fabricated to provide visibility into its interior as shown in Figure 4.9. Cut to size and molded over a form with heated acrylic, it was shaped and sealed securely for durability as shown in Table 4.4.

Table 4.4

Transparent Chamber Cylinder

Sr #	**Part Name**	**Quantity**	**Size** (L x D x T)
1	Chamber Cylinder	1	14.4 cm x 14.5cm x 3mm

Figure 4.9 Acrylic Sheet Molding

Chapter 5

Electrical Circuitry

Sensors & Components

Table 5.1 listing all the sensors and components used in the system.

Table 5.1

Sensor & Components

Sr #	Component	Quantity	Use
1	BMP 280	1	Ambient Pressure, Temperature & Altitude
2	ACS 712	2	Power calculation
3	5V Relay	1	Over heat shut-off
4	MAX6675	1	Contact type - temperature measurement
5	LM35	2	Air temperature measurement
6	HX710B	2	Flow type – pressure measurement
7	BTS7960	1	DC motor driver
8	Servo motor	2	Variable nozzle control
9	RPM Sensor	1	RPM measurement
10	XL 4015	1	Step down voltage converter
11	DC 775 Motor	1	Compressor Impeller driver
12	Generator Motor	1	Turbine Wheel driver
13	Arduino Mega	1	Data Acquisition
14	ESP 32	1	Wi-Fi Module
15	Buzzer	1	Overheat warning
16	Toggle Switch	4	Sensor, servo & motor control
17	Potentiometer	2	Servo & motor control
18	Power Button	1	System power control

Block Diagram

The block diagram as shown in Figure 5.1 illustrates two dotted boxes: one containing all sensors powered by the XL 4015 DC step-down voltage converter, adjusted to either 5V or 3.3V as per sensor requirements. The second dotted box indicates that the ESP32, Arduino Mega, and motor driver operate directly on 12V power. Blue lines represent data transmitted from sensors to the microcontroller, while red lines indicate power distribution. Orange lines signify control data wiring, green lines denote commands sent by the microcontrollers upon instruction, and purple arrows depict data sent online for visualization purposes.

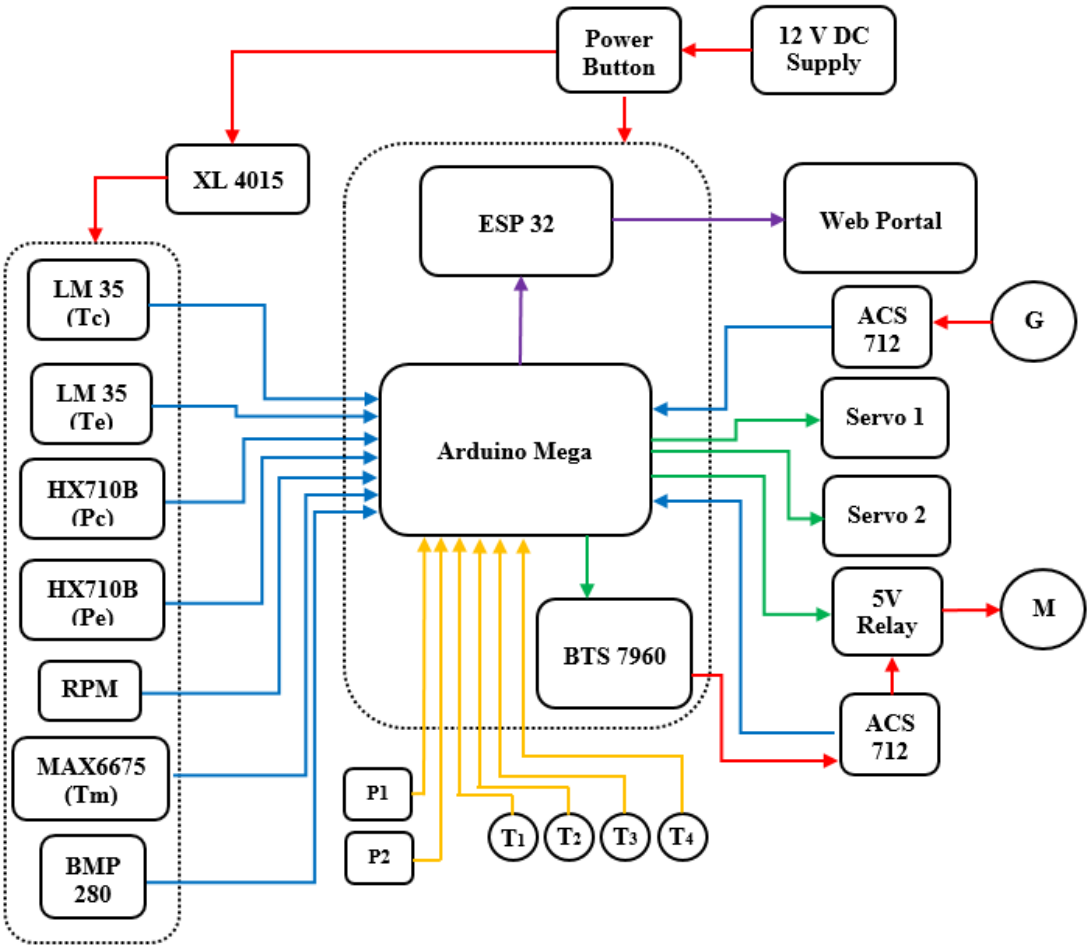

Figure 5.1 Block Diagram

Schematic Diagram

The schematic diagram shows the pin placements of each sensor and component in the electrical system as shown in Figure 5.2. The red lines represent the power connections, while the black lines indicate the ground connections. All other colors in the diagram represent data transfer pathways, ensuring clear and efficient communication between components.

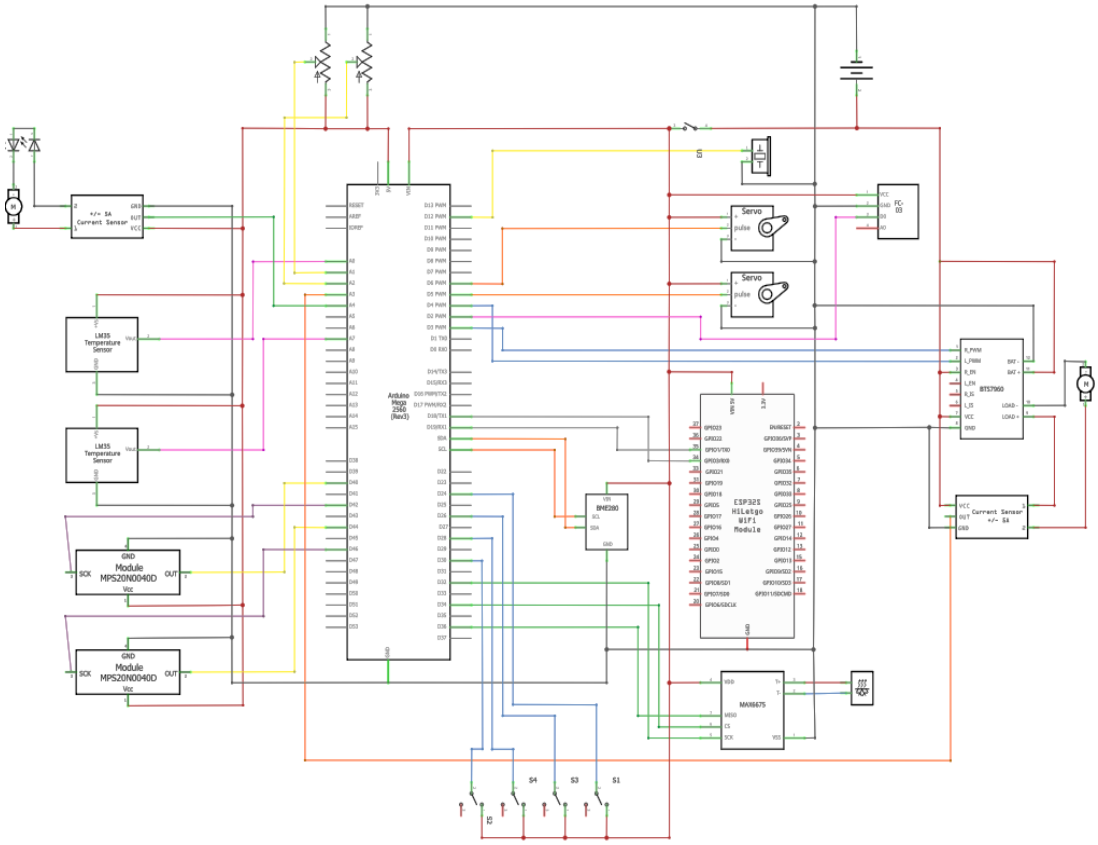

Figure 5.2 Schematic Diagram

Pin Configurations

The Table 5.2 below lists all the pin placements of each component and sensor, providing essential information for the assembly of the data acquisition box. This detailed reference will help ensure accurate and efficient wiring during the setup process.

Table 5.2

Pin Configurations

Sr#	Component /Sensor	Pin Name	Connection Type
1	K- Type Temp. Sensor (MAX 6675) (Tm)	thermoDO1	Digital Pin 36
		thermoCS1	Digital Pin 34
		thermoCLK1	Digital Pin 32
2	Relay	rly1	Digital Pin 9
3	Buzzer	buz	Digital Pin 12
4	Servo 1	Servo1	Digital Pin 5
5	Servo 2	Servo2	Digital Pin 6
6	BMP 280 (Ta, Pa)	SDA	I2C (A4)
		SCL	I2C (A5)
7	Toggle Switch 1	B1_Pin	Digital Pin 24
8	Toggle Switch 2	B2_Pin	Digital Pin 26
9	Toggle Switch 3	B3_Pin	Digital Pin 28
10	Toggle Switch 4	B4_Pin	Digital Pin 30
11	DC Motor RPWM Output	RPWM_Output	Digital Pin 3
12	DC Motor LPWM Output	LPWM_Output	Digital Pin 4
13	Sensor Pin	sensor_pin	Digital Pin 2
14	Temperature Sensor 1 (Tc)	T_S	Analog Pin 0
15	Temperature Sensor 2 (Te)	T_S1	Analog Pin 7
16	Potentiometer 1 (RPM)	pot_1pin	Analog Pin 1
17	Potentiometer 2 (Nozzle Angle)	pot_2pin	Analog Pin 2
18	Motor Current Sensor	currentPin	Analog Pin 3
19	Generator Current Sensor	currentPin1	Analog Pin 4
20	DC Voltage Sensor	DCvoltPin	Analog Pin 5
21	Ground Voltage Sensor	GvoltPin	Analog Pin 6
22	HX710 Pressure Sensor (Pc)	OUT	Digital Pin 40
		CLK	Digital Pin 42
23	HX710 Pressure Sensor (Pe)	OUT	Digital Pin 44
		CLK	Digital Pin 46
24	Nodemcu ESP 32	TX0	TX 1
		RX0	RX 1

Wiring

The wiring process started by soldering the microcontroller to a Vero board for stability as shown in Figure 5.3. Sensor attachment points were strategically left and soldered underneath for a tidy, professional appearance and organized component management.

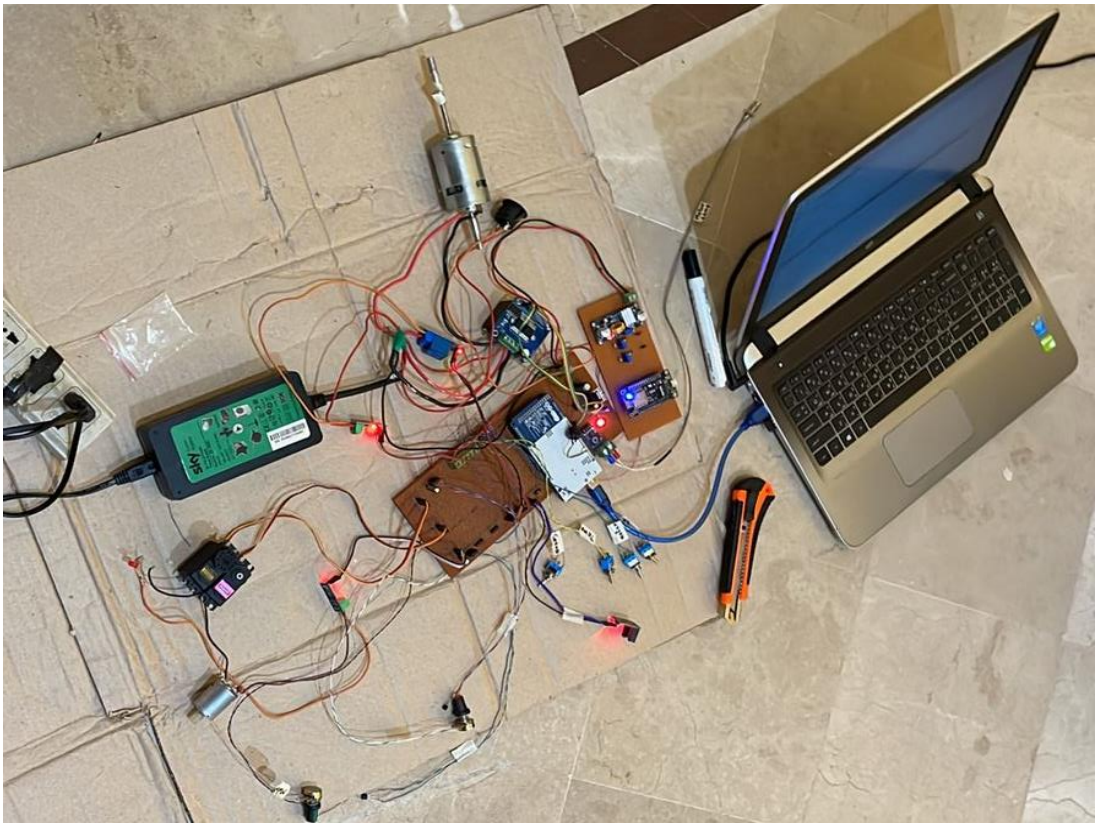

Figure 5.3 Wiring process

A second Vero board was soldered to accommodate the XL4015 voltage step-down converter and ESP32 module as shown in Figure 5.3. Sensors were then meticulously attached to designated points on the Vero board as shown in Figure 5.4, ensuring secure integration before programming the Arduino Mega microcontroller for software development and testing.

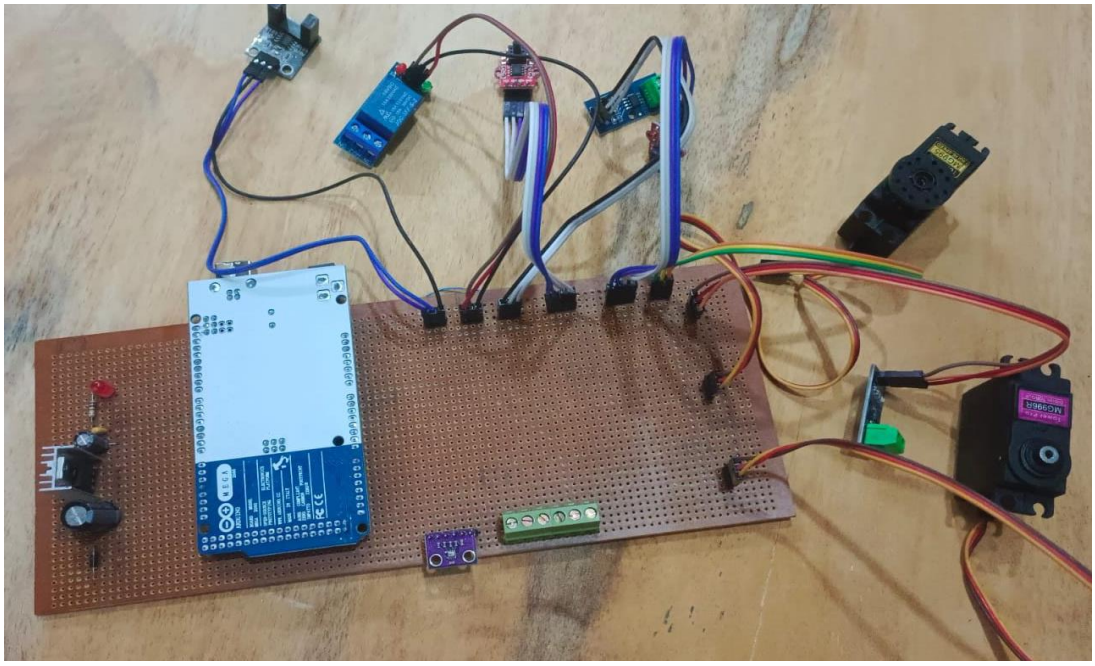

Figure 5.4 Sensor Attached to Vero board

Programming

Micro-controller (Arduino Mega)

The code imports necessary libraries for sensor communication and control. It specifies Arduino pins as shown in Table 5.2 for sensors and actuators. "Set Value" is crucial, monitoring motor temperature (Tm) to trigger protection actions if exceeded. In "setup()", serial communication and sensor connections are configured. "Loop()" reads temperatures, pressures, calculates RPM and efficiency, triggers protections for Tm. Data is printed for debugging and sent to ESP32 via Serial3 for online processing.

Wi-Fi Module (ESP 32)

The ESP32 first connects to a Wi-Fi network named "Sameer's iPhone" with a predefined password, enabling it to send data over the internet. It uses pins 18 and 19 for serial communication with the Arduino Mega. The ESP32 connects to a Firebase database at "testfb-24b31-default-rtdb.firebaseio.com" using an authentication key for secure data transfer.

The ESP32 continuously checks for messages from the Arduino Mega. Upon receiving a message, it identifies the data type (temperature, RPM, etc.) from the starting letter (A to P) and extracts the corresponding float value. It then sends this value to Firebase, labeling it appropriately (e.g., "Chamber Temperature" or "RPM"). This process ensures that all data is stored and labeled in Firebase for later use and analysis.

Web Portal Development

A third-party software specialist developed the web portal as shown in Figure 5.5, using Firebase data. Specifications were provided for various graphs in Table 5.3, depicting data with RPM and Time as independent variables on the X-axis.

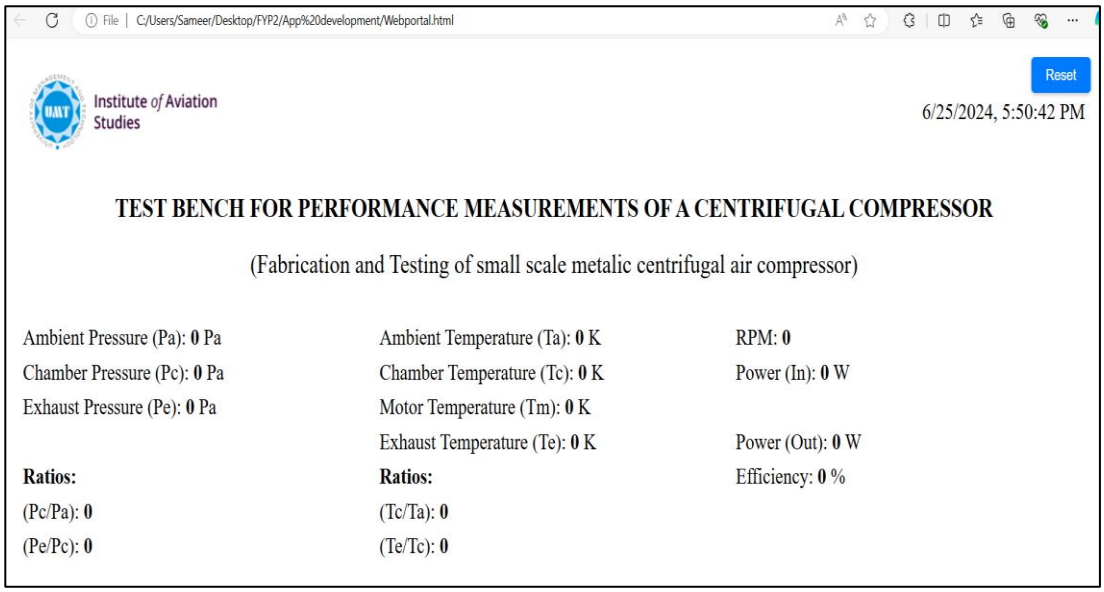

Figure 5.5 Web portal Layout

Table 5.3

Graphical Visualization on Web portal

Sr #	Graphs	X-Axis	Y-Axis
1	Pc vs RPM	RPM	Chamber Pressure
2	Pe vs RPM	RPM	Exhaust Pressure
3	Tc vs RPM	RPM	Chamber Temperature
4	Te vs RPM	RPM	Exhaust Temperature
5	Tm vs RPM	RPM	Motor Temperature
6	Efficiency vs RPM	RPM	Efficiency
7	Pc vs Time	Time	Chamber Pressure
8	Pe vs Time	Time	Exhaust Pressure
9	Tc vs Time	Time	Chamber Temperature
10	Te vs Time	Time	Exhaust Temperature
11	Tm vs Time	Time	Motor Temperature

Chapter 6

Assembly

The engine assembly integrated 14 components from Table 4.1, including 3D-printed parts and the acrylic chamber cover as shown in Figure 4.9. Initial focus was on the nozzle assembly with components like the turbine wheel, generator motor, nozzle holder, and 12 blades as shown in Figure 6.1. Exhaust temperature and pressure sensors were then positioned after the turbine wheel (Figure 6.1).

Figure 6.1 Actual Nozzle Assembly

Next, Figure 6.2 illustrates how the motor holder accommodates the DC 775 motor, RPM sensor, and encoder within the assembly. The contact-type temperature sensor and the chamber temperature sensor are attached to the same motor holder assembly as shown in Figure 6.3. And Figure 6.4 depicts the placement of the chamber pressure sensor in the diffuser.

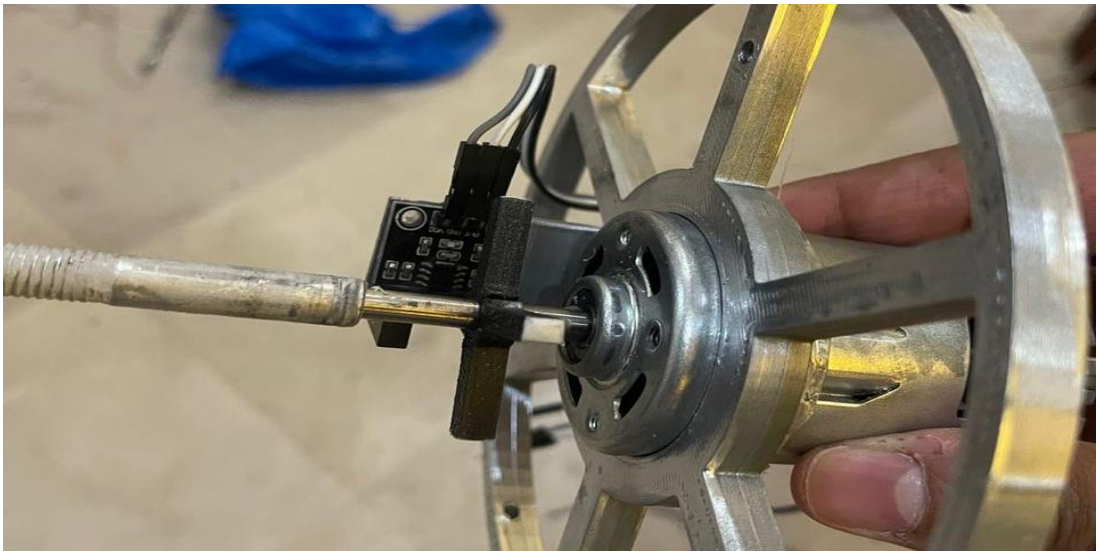

Figure 6.2 Actual RPM Sensor & Motor Placement

Figure 6.3 Actual K-type and Chamber Temp. Sensor Placement

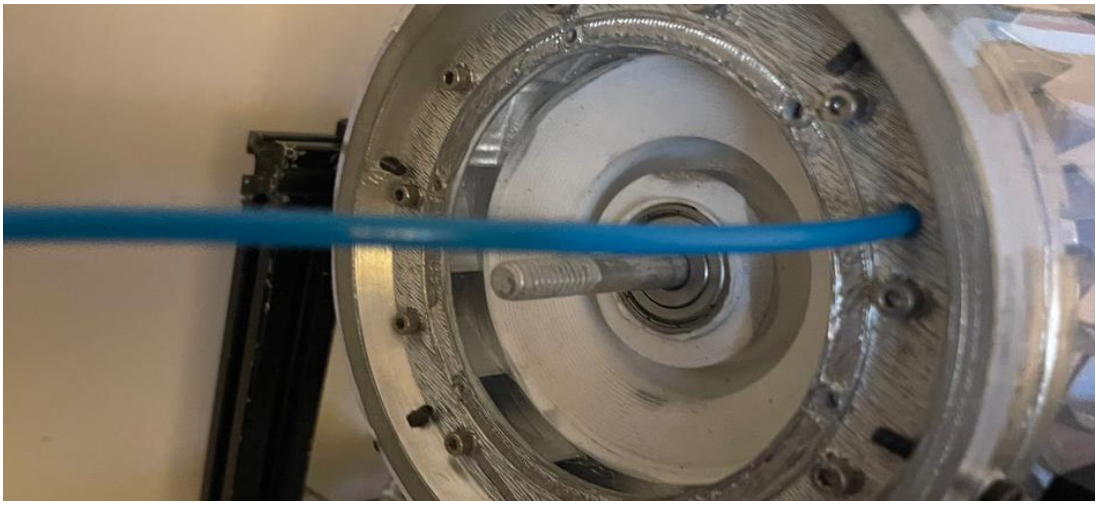

Figure 6.4 Actual Chamber Pressure Tube Placement

The entire assembly, including all components described in Chapter 4 and 5, were mounted onto the board as shown in Figure 6.5. The DC motor connected to the centrifugal compressor was balanced on a bearing stuck into the diffuser. The Micro jet engine was held with M3 bolts along with M12 bolts to hold the micro jet engine with clamps.

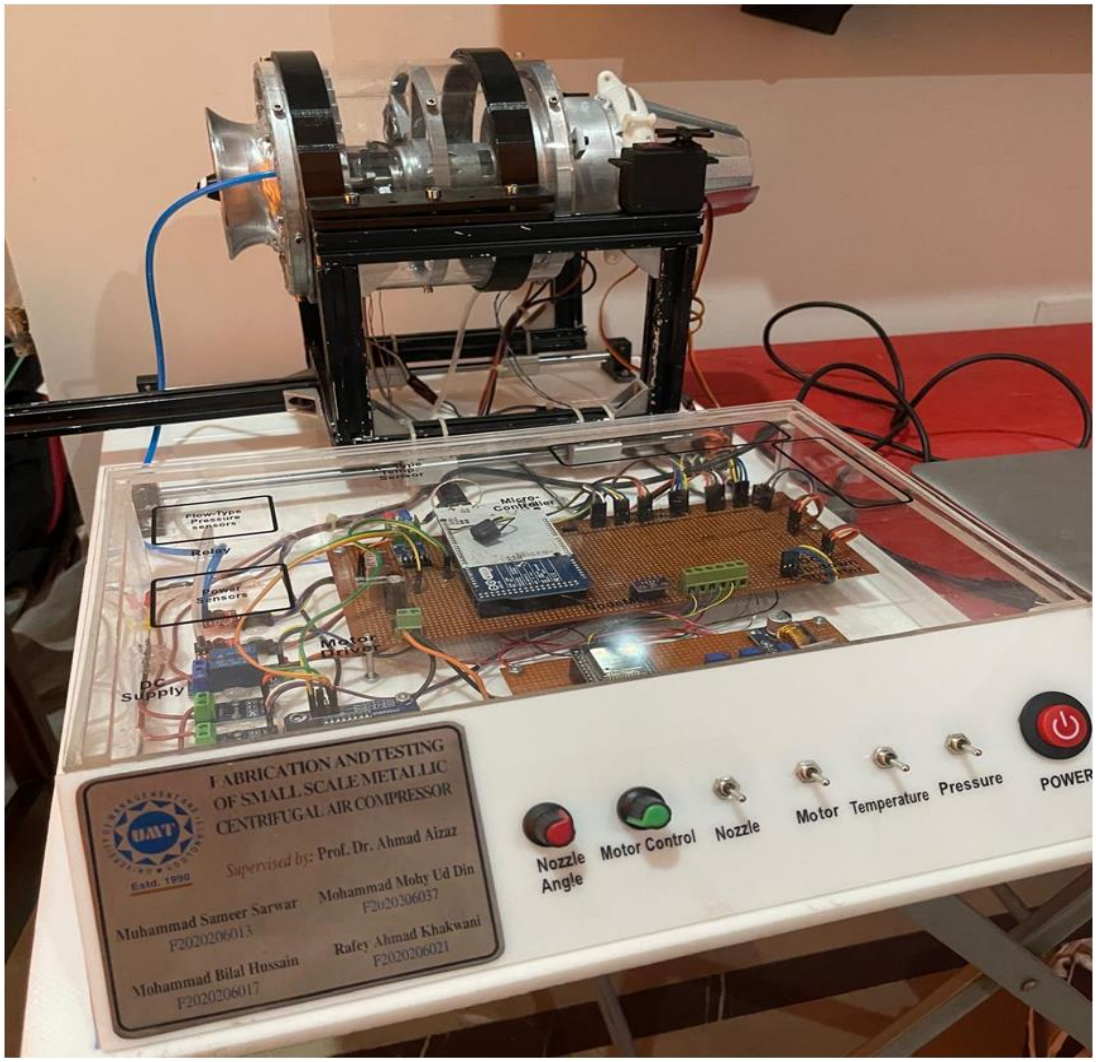

Figure 6.5 Actual completed Assembly

Chapter 7

Testing

Normal Condition

The testing phase evaluated the micro jet engine's performance and operational characteristics, focusing on compression pressure ratio and compression temperature ratio across RPMs from 1000 to 6000. Parameters were monitored and recorded, summarized in Table 7.1 below.

Table 7.1

Normal Condition Test Readings

Sr#	**RPM (± 80)**	**Pc** (Pascal) **(± 2500)**	**Tc** (Kelvin) **(± 0.60)**	**Pe** (Pascal) **(± 1500)**	**Te** (Kelvin) **(± 0.45)**	**CPR (±0.002)**	**CTR (±0.002)**
1	**0**	99889	309.15	99889	304.15	1.023	1.003
2	**1037**	99889	309.15	99889	304.15	1.023	1.003
3	**1512**	99895	309.15	99895	304.15	1.023	1.003
4	**2042**	103800	309.54	100408	304.18	1.063	1.004
5	**2521**	107000	310.67	101738	304.18	1.096	1.008
6	**3011**	111370	311.19	103458	304.18	1.141	1.010
7	**3562**	115240	311.67	104278	304.17	1.180	1.011
8	**4077**	119324	312.71	106398	304.19	1.222	1.015
9	**4524**	123805	313.44	107018	304.18	1.268	1.017
10	**5019**	127395	313.67	108738	304.18	1.305	1.018
11	**5585**	131973	314.25	110378	304.19	1.352	1.020
12	**6005**	134175	314.50	111397	304.19	1.395	1.020

The tests were conducted in a controlled, air-conditioned environment. It's important to note that readings may vary in different settings due to factors like ambient temperature and humidity. Ambient pressure was measured at 97622.01 Pascal's and ambient temperature at 308.19 Kelvin, influencing calculations of compression pressure ratio (CPR) and compression temperature ratio (CTR). Figures

7.1-7.4 depict how chamber pressure (Pc), chamber temperature (Tc), exhaust pressure (Pe), exhaust temperature (Te), CPR, and CTR change with increasing RPMs, providing visual insights into compressor performance.

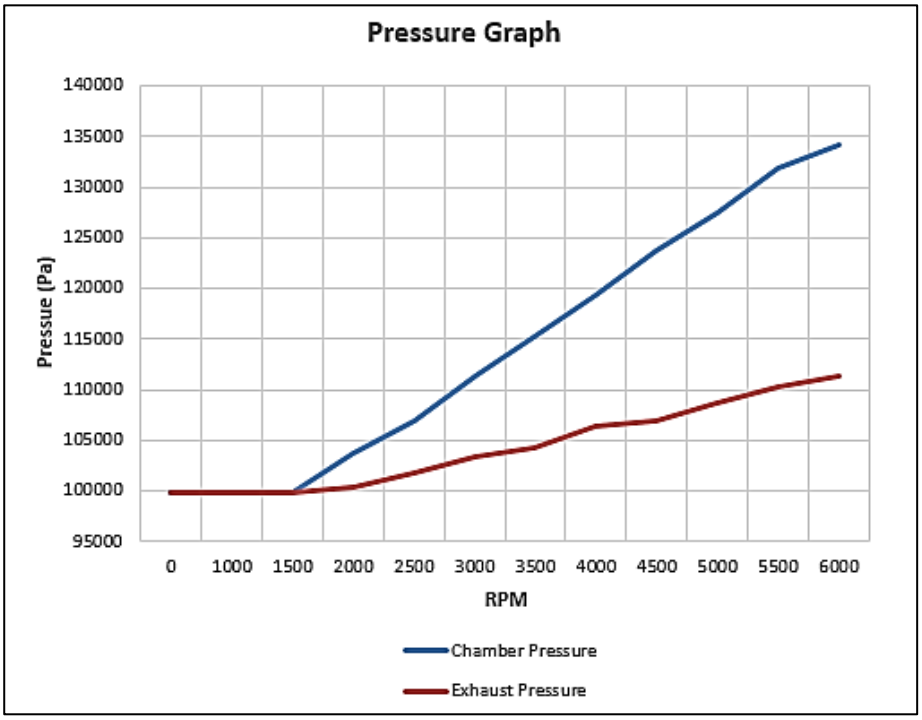

Figure 7.1 Pressure Change vs RPM at Normal Condition

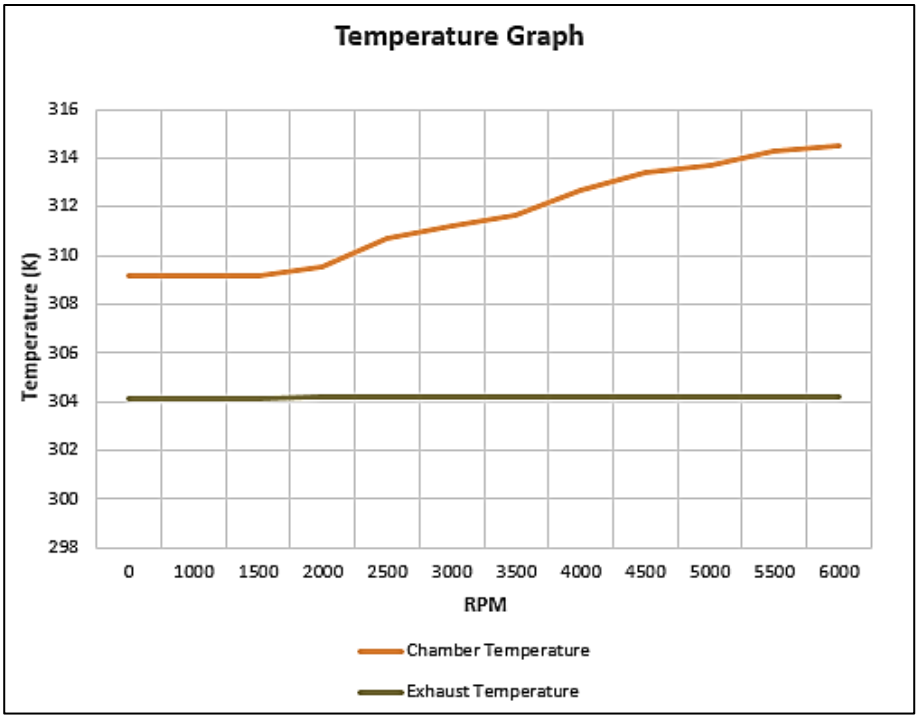

Figure 7.2 Temperature Change vs RPM at Normal Condition

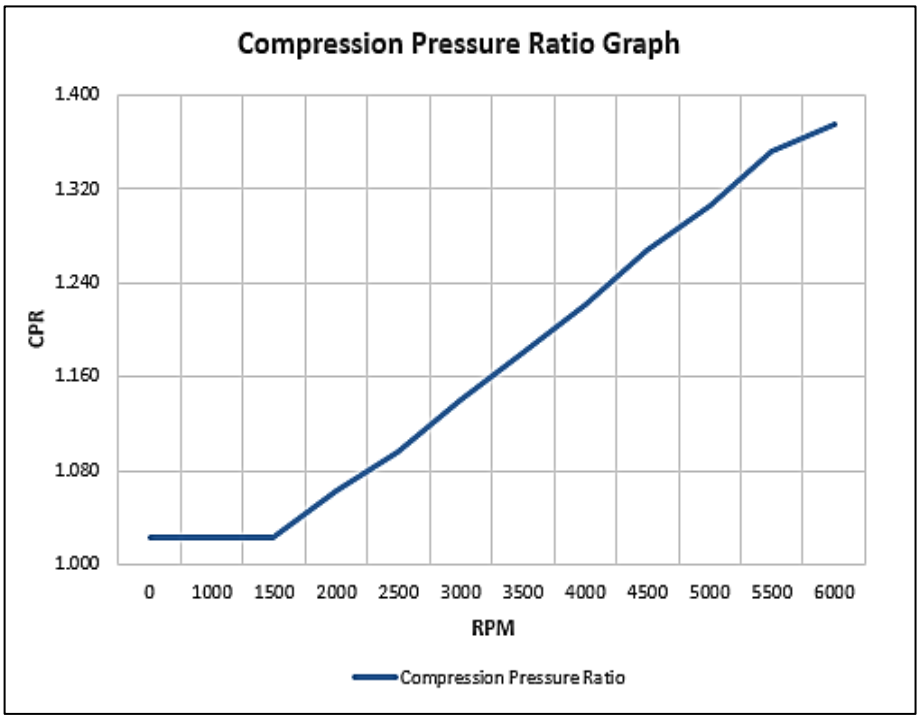

Figure 7.3 CPR Change vs RPM at Normal Condition

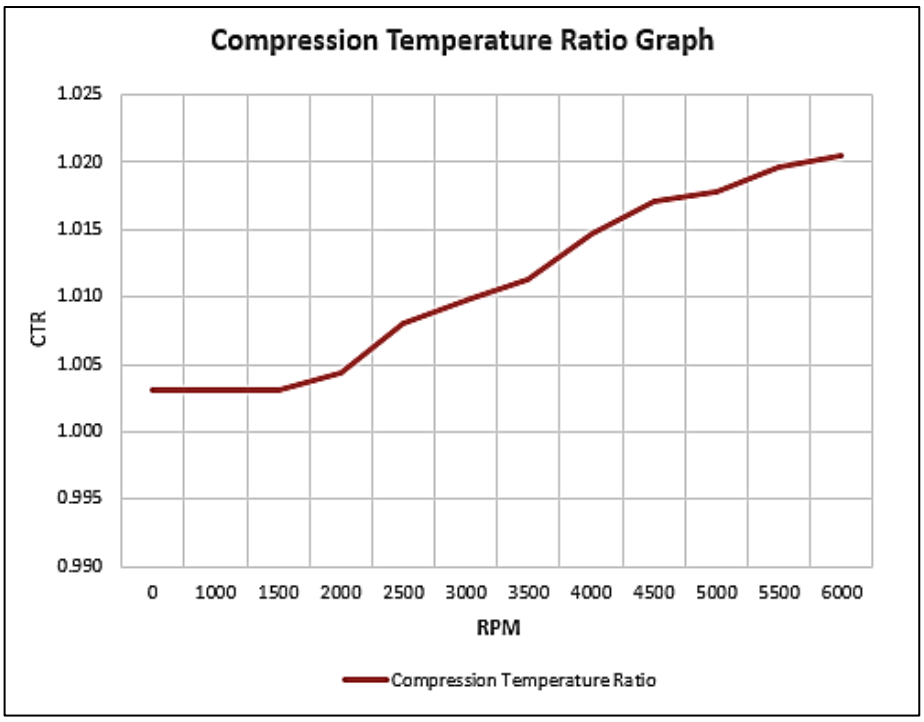

Figure 7.4 CTR Change vs RPM at Normal Condition

Table 7.2 shows the temperature of the motor (Tm), power, and efficiency values recorded during the test conducted at different RPMs.

Table 7.2

Additional Normal Condition Test Readings

Sr#	**RPM** **(± 80)**	**Tm** (Kelvin) **(± 0.45)**	**Pin** (W) **(± 6.25)**	**Pout** (W)	**Efficiency** (%)
1	0	309.15	0	0	0
2	1021	309.15	0.61	0	0
3	1534	309.15	1.18	0	0
4	2011	309.21	1.74	0	0
5	2521	309.67	2.37	0	0
6	3038	310.14	3.18	0	0
7	3542	310.33	3.54	0	0
8	4071	310.54	4.25	0	0
9	4512	310.8	4.66	0	0
10	5078	311.51	5.52	0	0
11	5510	311.82	5.94	0	0
12	6021	312.44	6.17	0	0

The Figures 7.5-7.7 shows the temperature of the motor, the power generated, the power consumed, and the efficiency graphs from the test conducted. The graphs illustrate how the motor's temperature, power generation and consumption, and overall efficiency vary with the RPM.

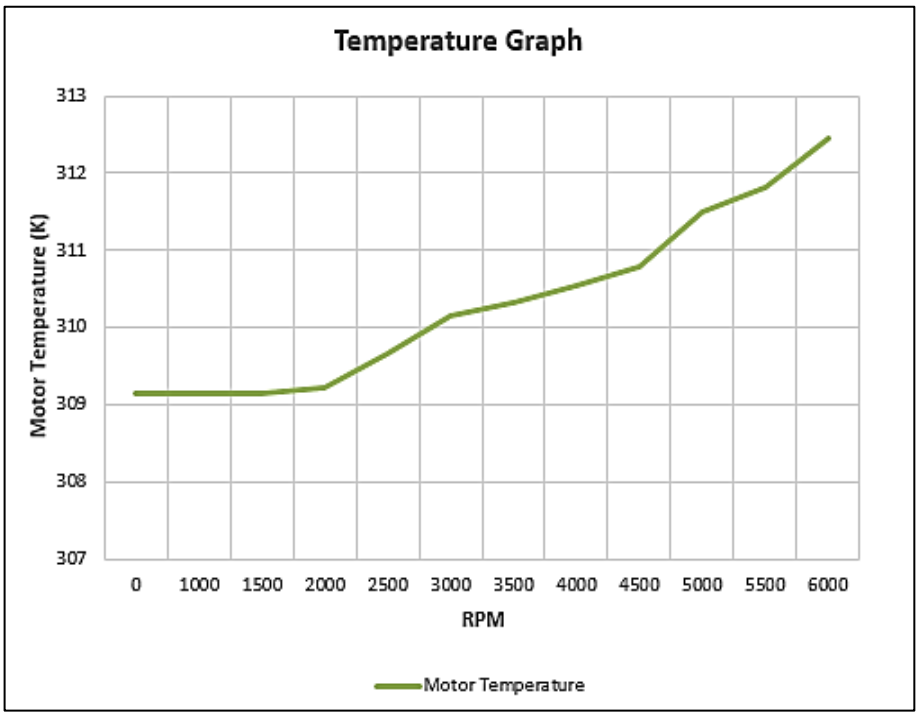

Figure 7.5 Temperature Change vs RPM at Normal Condition

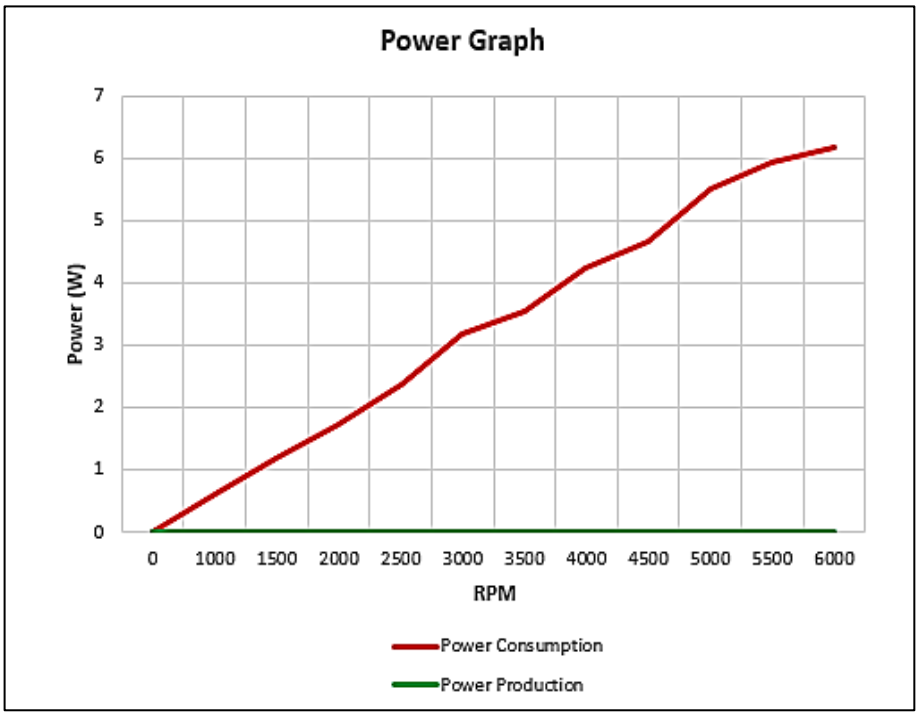

Figure 7.6 Power vs RPM at Normal Condition

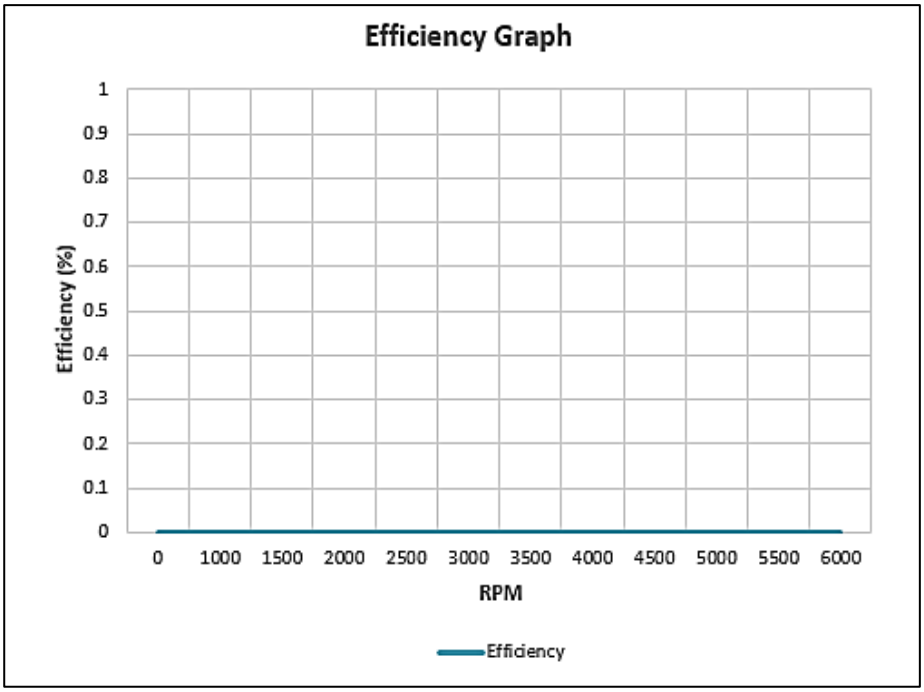

Figure 7.7 Efficiency vs RPM at Normal Condition

Stall Condition

The next test aimed to observe the stalling conditions of the centrifugal compressor. This test was conducted at a room temperature of 307.15 Kelvin and an ambient pressure of 97622.01 Pascal's. The values achieved from the test are in Table 7.3 and the Figure 7.8 -7.11 depicts the graphs.

Table 7.3

Stall Condition Test Readings

Sr#	**RPM (± 80)**	**Time**	**Pc** (Pascal) **(± 2500)**	**Tc** (Kelvin) **(± 0.60)**	**CPR (±0.002)**	**CTR (±0.002)**
1	0	7:34:29	98111	307.1	1.01	1.00
2	1010	7:35:42	98121	307.1	1.01	1.00
3	1521	7:37:10	98134	307.15	1.01	1.00
4	2038	7:40:25	103710	309.21	1.06	1.01
5	2542	7:41:37	107440	310.17	1.10	1.01
6	3000	7:44:21	111130	310.89	1.14	1.02
7	3508	7:46:38	115240	311.21	1.18	1.02
8	4071	7:47:10	119324	311.72	1.22	1.02
9	**3010**	**7:48:29**	**110420**	**311.35**	**1.13**	**1.02**
10	**2001**	**7:50:33**	**104534**	**310.84**	**1.07**	**1.02**
11	2508	7:51:02	106121	310.32	1.09	1.01
12	3021	7:52:48	109430	310.64	1.12	1.01

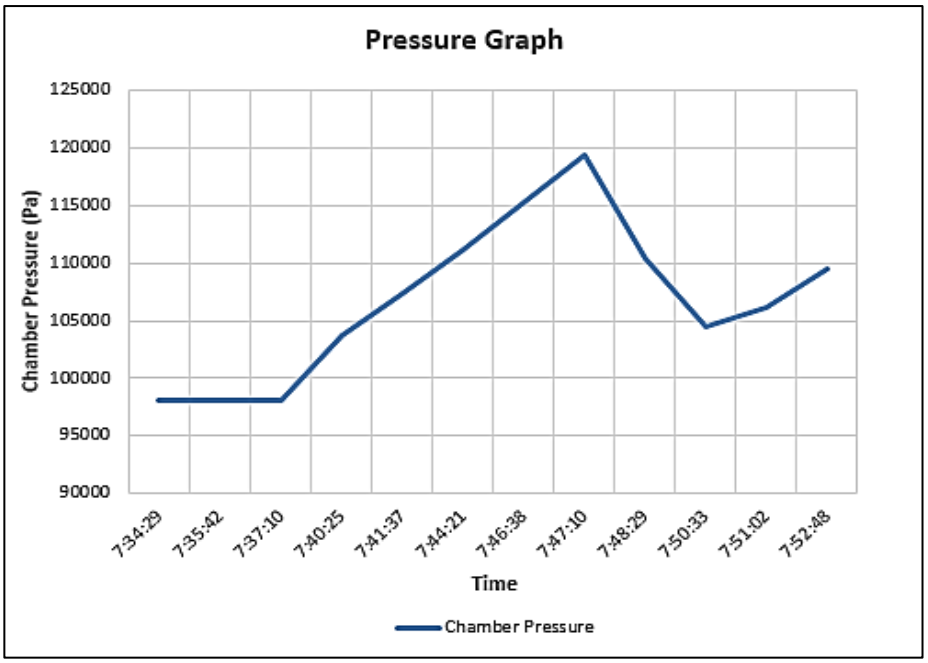

Figure 7.8 Pressure Change vs Time at Stall Condition

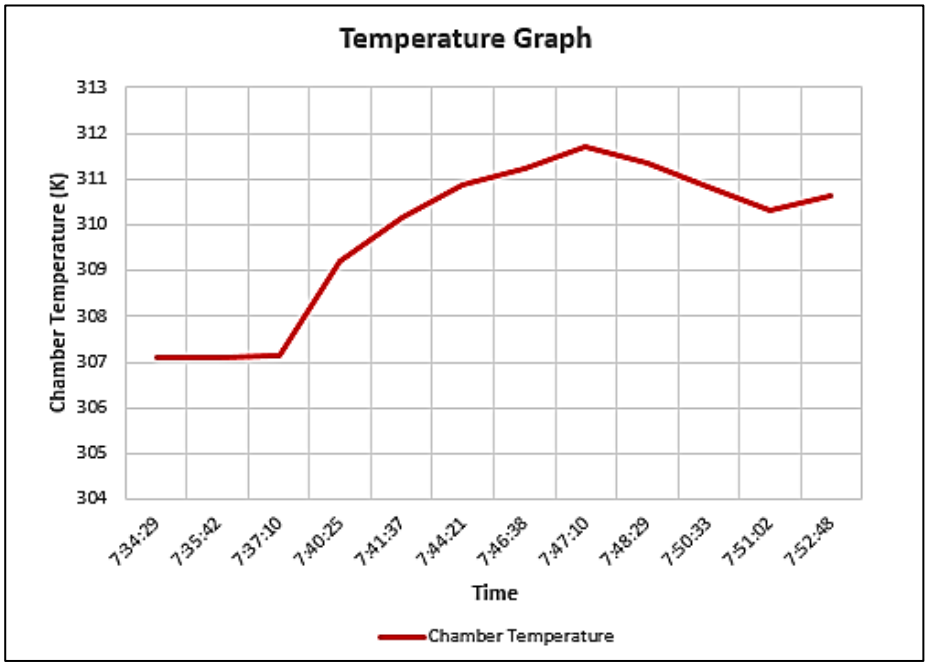

Figure 7.9 Temperature Change vs Time at Stall Condition

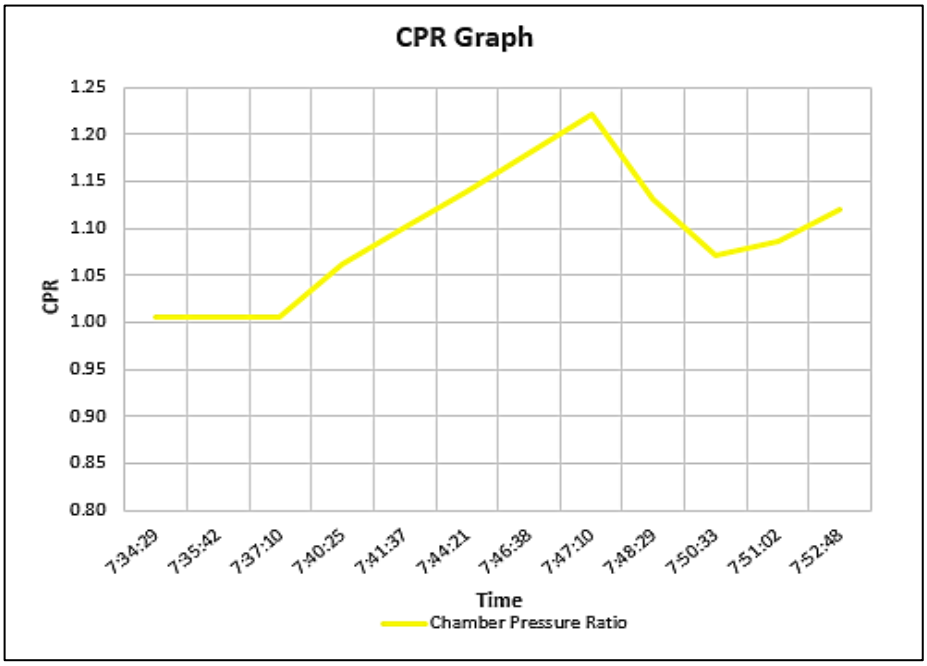

Figure 7.10 CPR Change vs Time at Stall Condition

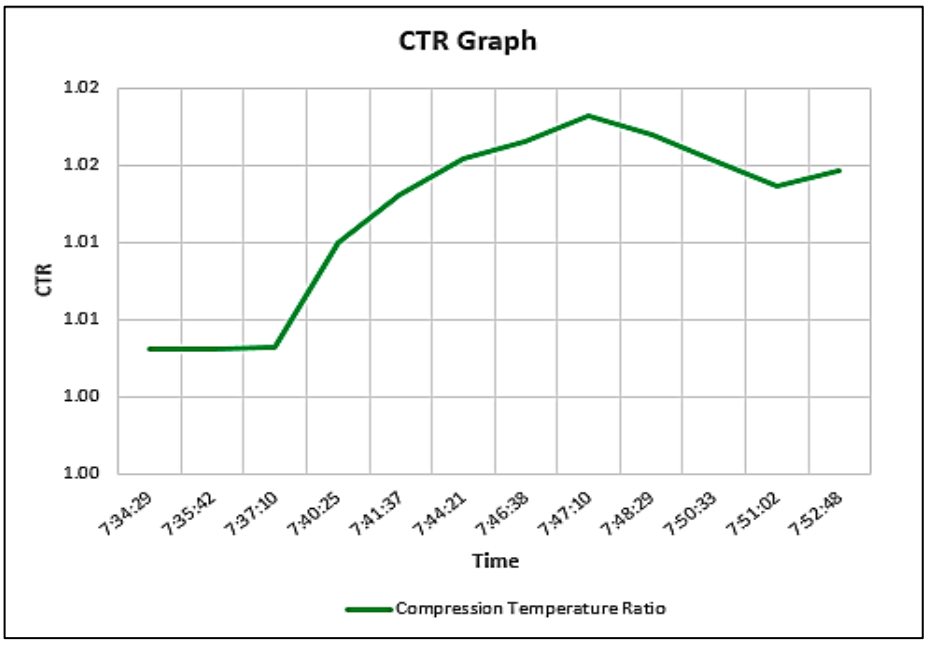

Figure 7.11 CTR Change vs Time at Stall Condition

Surge Condition

This test observed the surge conditions of the centrifugal compressor. This test was conducted at a room temperature of 307.15 Kelvin and an ambient pressure of 97622.01 Pascal's. The values are shown in Table 7.4, and the graphs are depicted in Figures 7.12 to 7.15.

Table 7.4

Surge Condition Test Readings

Sr#	**RPM**	**Time**	**Pc** (Pascal)	**Tc** (Kelvin)	**CPR**	**CTR**
1	0	8:05:29	98111	307.1	1.01	1.00
2	1012	8:06:42	98121	307.1	1.01	1.00
3	1514	8:08:10	98212	307.15	1.01	1.00
4	2021	8:09:25	103640	309.21	1.06	1.01
5	2514	8:10:37	107921	310.17	1.11	1.01
6	3035	8:15:21	111420	310.89	1.14	1.02
7	3541	8:16:38	115114	311.21	1.18	1.02
8	4000	8:17:10	119792	311.72	1.23	1.02
9	**2527**	**8:21:02**	**107321**	**311.31**	**1.10**	**1.02**
10	3007	8:22:48	110521	311.44	1.13	1.02
11	3521	8:23:38	114211	311.52	1.17	1.02
12	4015	8:25:10	119440	311.91	1.22	1.02

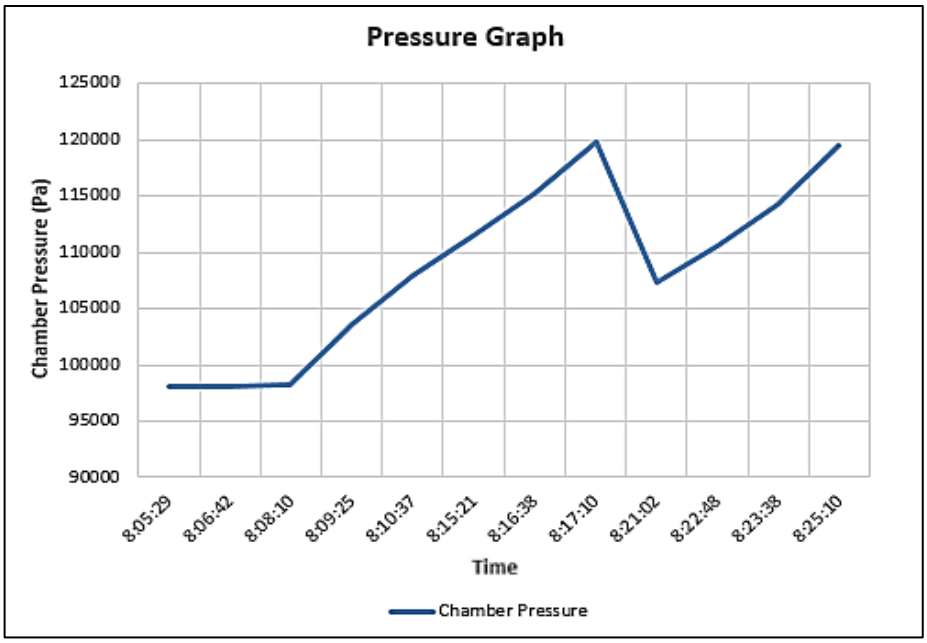

Figure 7.12 Pressure Change vs Time at Surge Condition

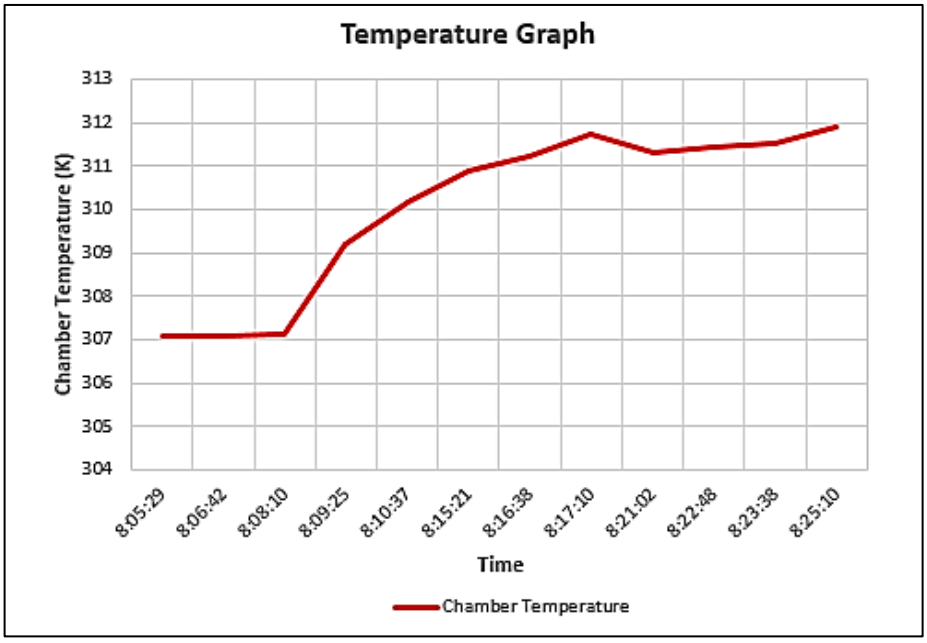

Figure 7.13 Temperature Change vs Time at Surge Condition

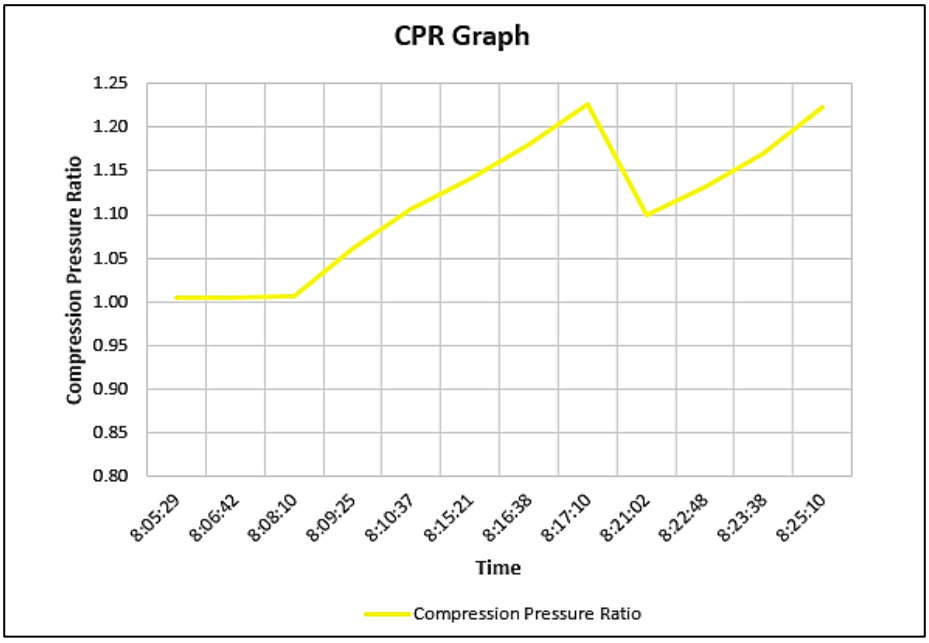

Figure 7.14 CPR Change vs Time at Surge Condition

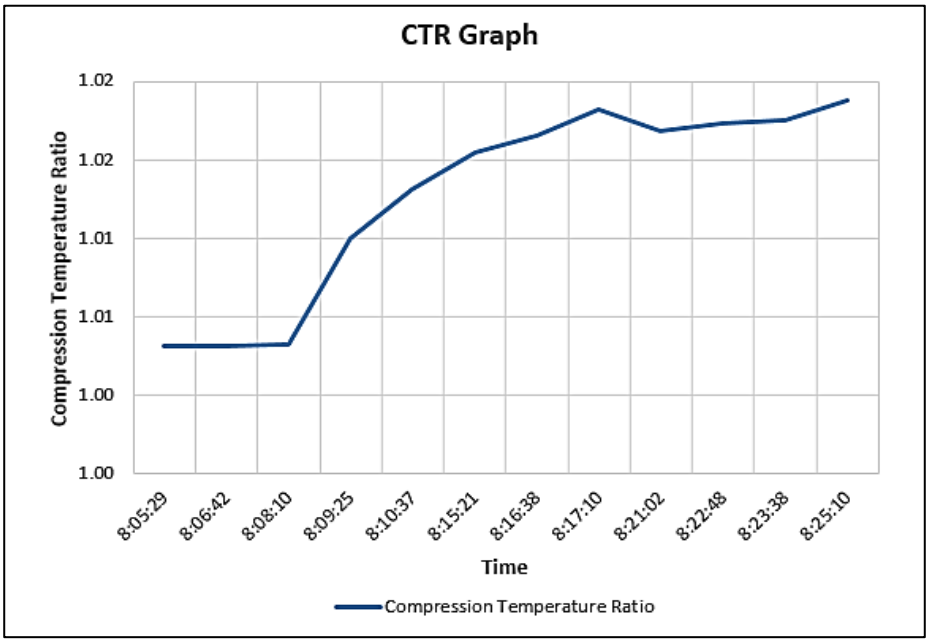

Figure 7.15 CTR Change vs Time at Surge Condition

Analysis

Standard Condition

Standard testing of the centrifugal compressor spanned RPMs from 0 to 6005. Chamber pressure peaked at 134175 Pa from 99889 Pa at 0 RPM, showing effective pressure increase. Chamber temperature rose to 314.50 K from 309.15 K, indicating heat generation. Exhaust pressure rose to 111397 Pa from 99889 Pa, reflecting air expulsion. Compression pressure ratio increased to 1.395 from 1.023, improving pressurization. Compression temperature ratio rose slightly to 1.020. Motor temperature increased to 312.44 K from 309.15 K, indicating heat generation. Power consumption by the DC 775 motor rose to 6.17 W from 0 W at 0 RPM. The generator motor connected to the turbine wheel did not generate power, suggesting insufficient chamber pressure. Efficiency remained at 0%, due to the absence of a combustion chamber.

Stall Condition

Stall testing on the centrifugal compressor assessed behavior across RPMs from 0 to 4071, with decreases and increases. Key parameters included chamber pressure (Pc) reaching 98111 Pa at 0 RPM, peaking at 119324 Pa at 4071 RPM, and dropping to 104534 Pa at 2001 RPM. The pressure drop indicates stall condition. Chamber temperature (Tc) rose to 311.72 K at 4071 RPM and settled at 310.64 K at 3021 RPM when stalling. CPR peaked at 1.22 at 4071 RPM, then slowly decreasing to 1.07 at 2001 RPM while CTR also decreased to 1.02 indicating stall conditions. Gradually increasing to 109430 Pa at 30021 RPM indicating normal functioning.

Surge Condition

Surge condition testing on the centrifugal compressor assessed its response to RPM changes from 0 to 4000. Key parameters like chamber pressure (Pc), chamber temperature (Tc), compression pressure ratio (CPR), and compression temperature ratio (CTR) were recorded. Results showed fluctuations in Pc from 98111 Pa to 119792 Pa, Tc from 307.1 K to 311.91 K, CPR from 1.01 to 1.23, and stable CTR at 1.00 to 1.02, the sudden drop in Pc to 107321 Pa and Tc 311.31 K at 2527 RPM. These values indicate the compressor surge conditions.

Sources of Errors

While measuring the parameters of the compressor, several possible errors affected the accuracy of the readings. These errors stemmed from various sources, including instrumentation, environmental factors, and the physical setup of the test stand. Instrumental errors were observed due to sensor calibration issues, where readings could drift over time due to unknown errors. Additionally, the sensors' slow response times were noted, which could fail to capture rapid changes in the parameters being measured

Environmental errors were also identified, such as fluctuations in ambient temperature or humidity levels, which could have impacted the accuracy of the sensors. Mechanical vibrations were another significant source of potential inaccuracies in the readings.

Issues related to installation and setup included potential leakages that could lead to incorrect readings, as well as poor insulation causing heat loss or gain. Heat transfer within a closed chamber, were affected by the heat generated by the motor, potentially resulting in higher sensor readings.

Chapter 8

Conclusion

The change from a dual-shaft to a single-shaft design in the micro jet engine has been pivotal, allowing the turbine wheel to rotate freely and providing measurements. The decision to 3D print all parts in only ABS was deemed unnecessary, so the structure was printed in PLA and PET-G along with ABS. The current setup, including the test stand, micro jet engine, and electronic box, provides a robust foundation for future enhancements. Despite encountering issues with airflow due to an oversized chamber, the project lays a solid groundwork for future advancements in micro jet engine technology with compressor impeller interchangeability capabilities.

Future Improvements

Future improvements for the micro jet engine setup include integrating a flow meter for precise efficiency calculations and adding a Venturi duct inside the chamber to optimize airflow dynamics and enhance turbine responsiveness. Upgrading to a more powerful motor capable of 30,000 RPM will increase the engine's output and expand its operational range. Additionally, refining the web portal to filter out erroneous data transmitted by the microcontroller is essential. This will ensure accurate graph plotting, reflecting genuine performance trends and enhancing the portal's utility for analysis.

REFERENCES

Bellis. (2019, 6 23). *ThoughtCo.* Retrieved 1 8, 2024, from https://www.thoughtco.com/history-of-the-jet-engine-4067905

Braembussche. (2019). *Design and Analysis of Centrifugal Compressors* (1st ed.). Hoboken: John Wiley & Sons Ltd.

GTEBuilders. (2020). *MW54*. Retrieved 1 8, 2024, from https://www.gtba.co.uk/engine_designs/mw54.htm

Hirndorf. (2013). *Very Small Gas Turbine Jet Engines.* Retrieved 1 8, 2024, from eucass.eu: https://rb.gy/erei97

Murphy, M. (2022, March 01). *MW54 Turbo-Prop Construction Manual.* Retrieved June 15, 2024, from http://totallyscrewedmachineshop.com/documents/turboprop_instructions_pt1.pdf

NASA. (2021, 5 13). *Centrifugal Compressor*. Retrieved 1 8, 2024, from https://www.grc.nasa.gov/www/k-12/airplane/centrf.html#:~:text=There%20are%20two%20main%20types,discussed%20on%20a%20separate%20slide.

NASM. (2022). *Whittle W.1X Engine*. Retrieved 1 9, 2024, from https://airandspace.si.edu/collection-objects/whittle-w1x-turbojet-engine/nasm_A19500082000

Paulsen. (1994). *Marine Engineering* (2nd ed.). Oxford: Butterworth-Heinemann.

Qairblogger. (2017). Centrifugal Air Compressor Controls And Basic Sizing. California: Q Air-California.

Sudheer. (2023, 4). Retrieved 1 8, 2024, from https://shorturl.at/Nrgrv

APPENDICES

APPENDIX A

Gantt chart & Costing

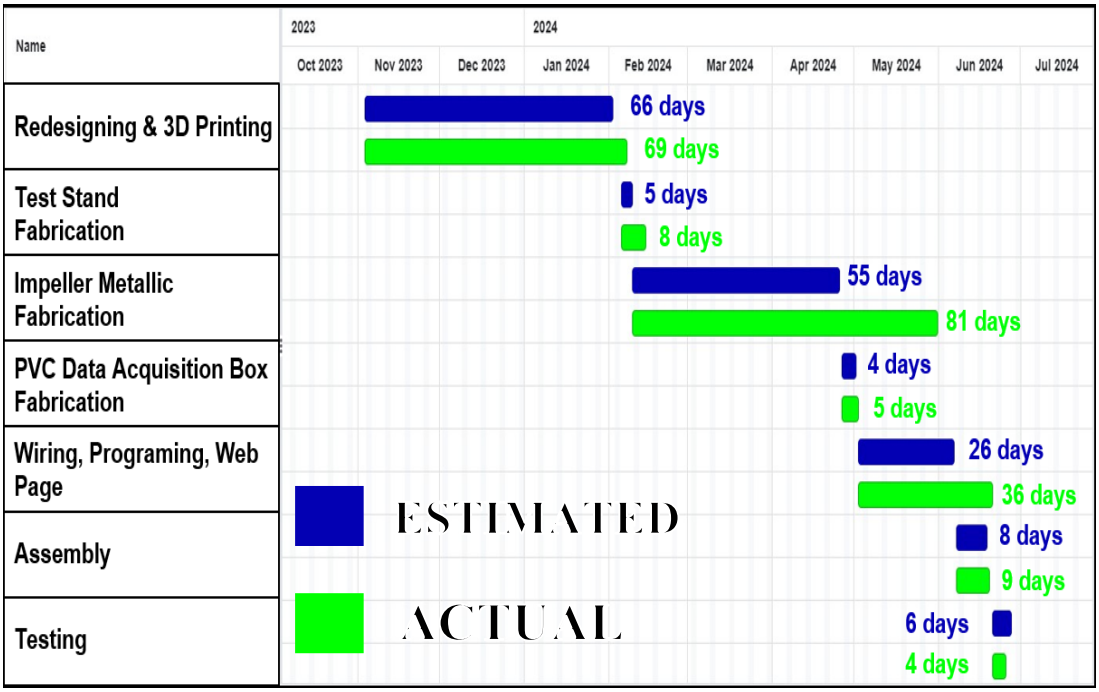

Gantt chart Timeline

Sr#	Task	Cost (PKR)
1	Prototype 3D printing	23,745 /-
2	Hardware	22,800 /-
3	Electronics	25,480 /-
4	3D printing (ABS, PET-G)	34,070 /-
5	Metallic fabrication	30,900 /-
6	Web portal development	20,000 /-
	Total	**156,995 /-**

Total Cost of Project

APPENDIX B

CAD DRAWINGS

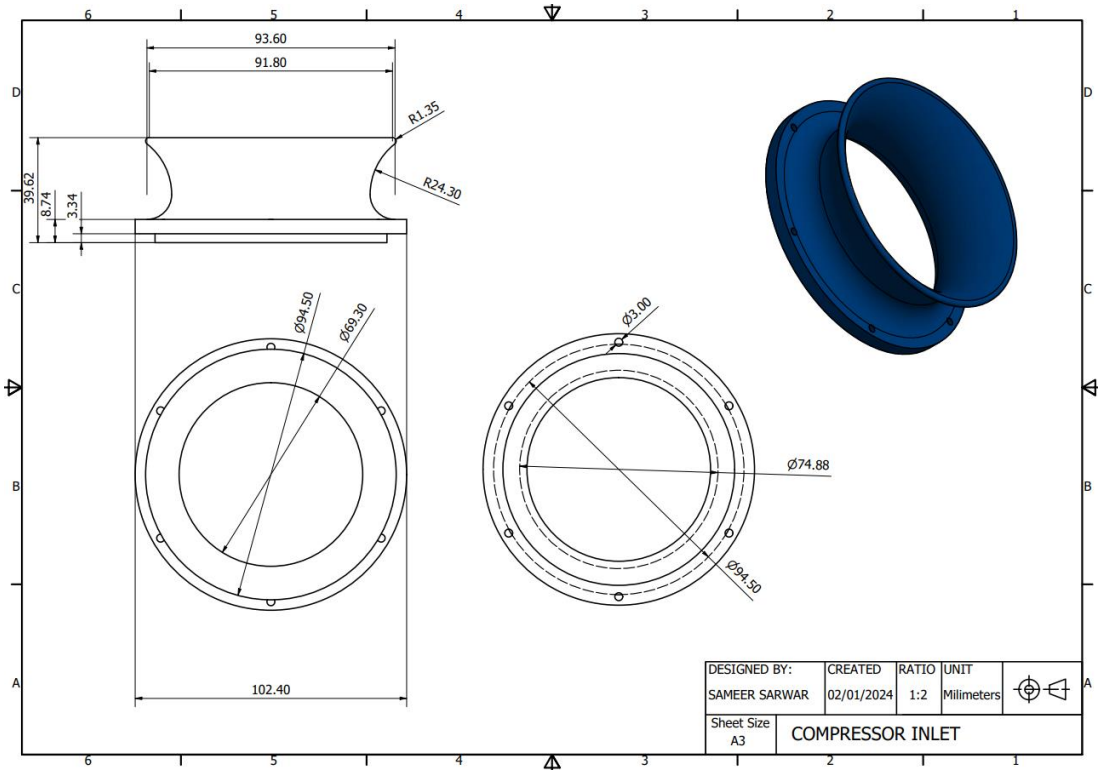

Compressor Inlet

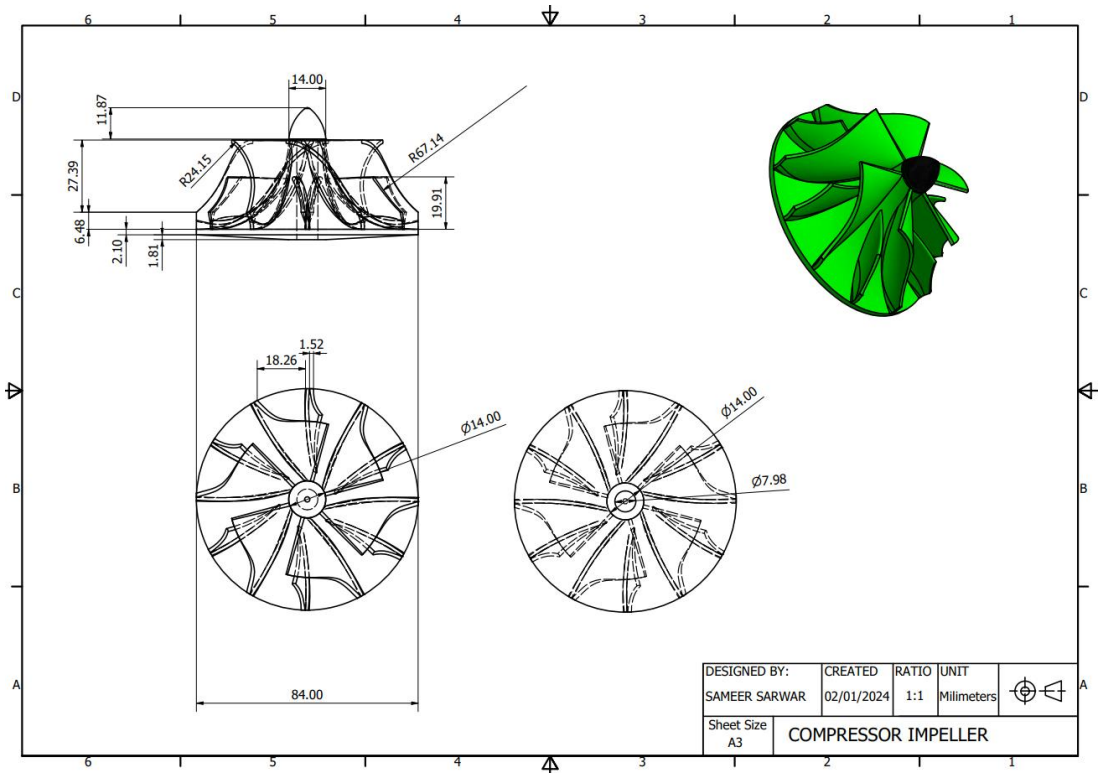

Compressor Impeller

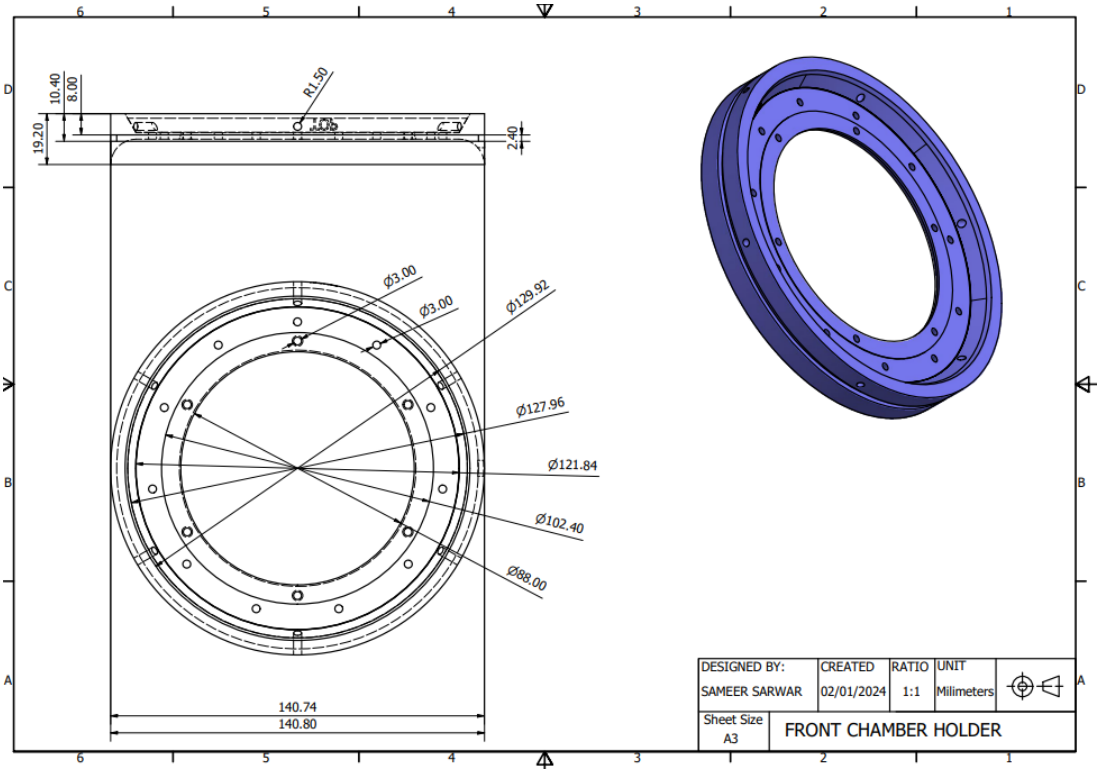

Front Chamber Holder

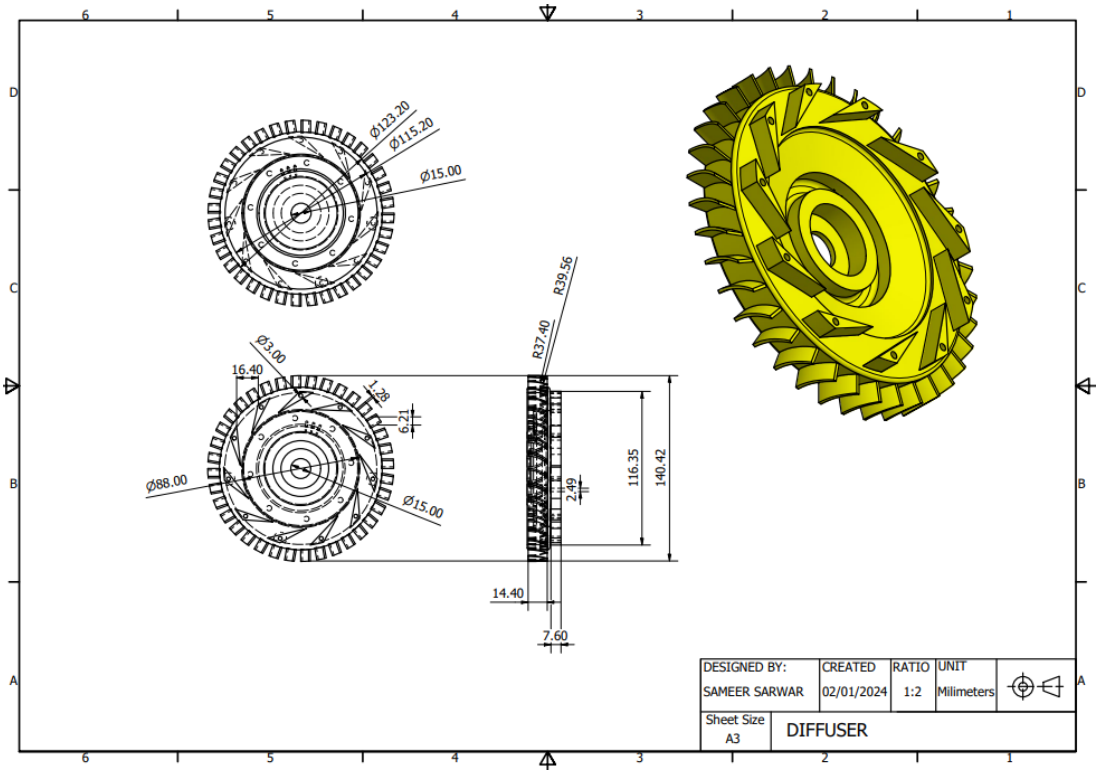

Diffuser

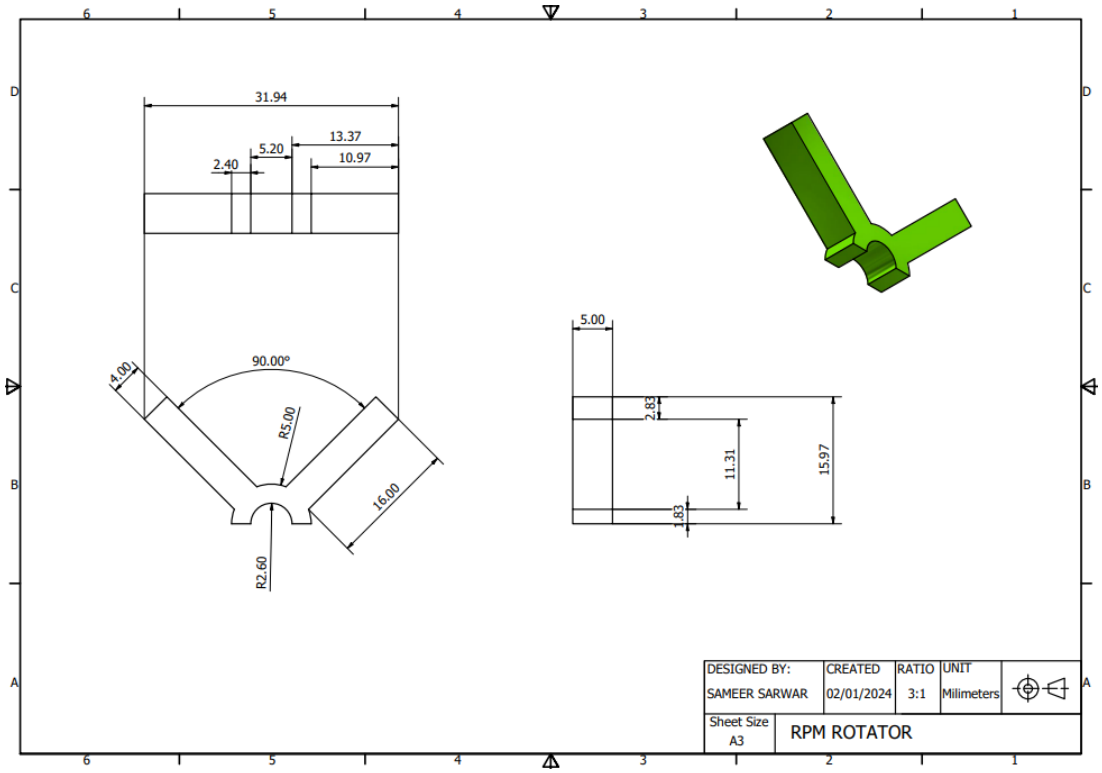

ROM Rotator Deflector (Encoder)

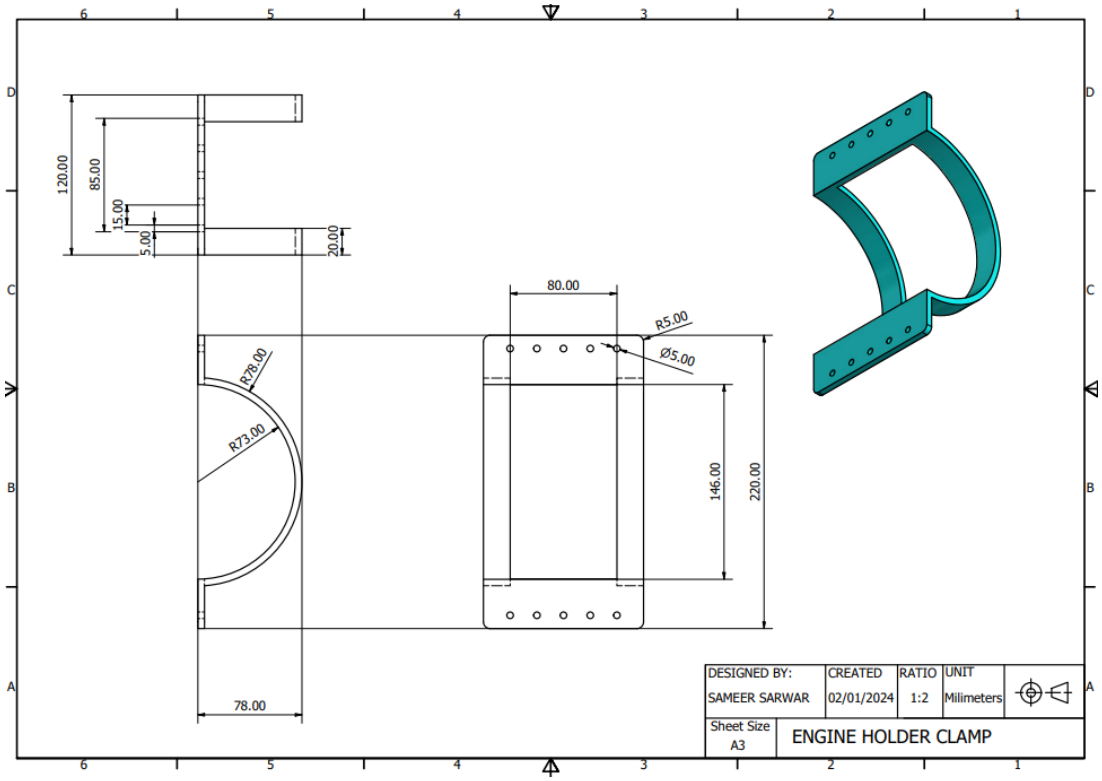

Engine Holder Clamp

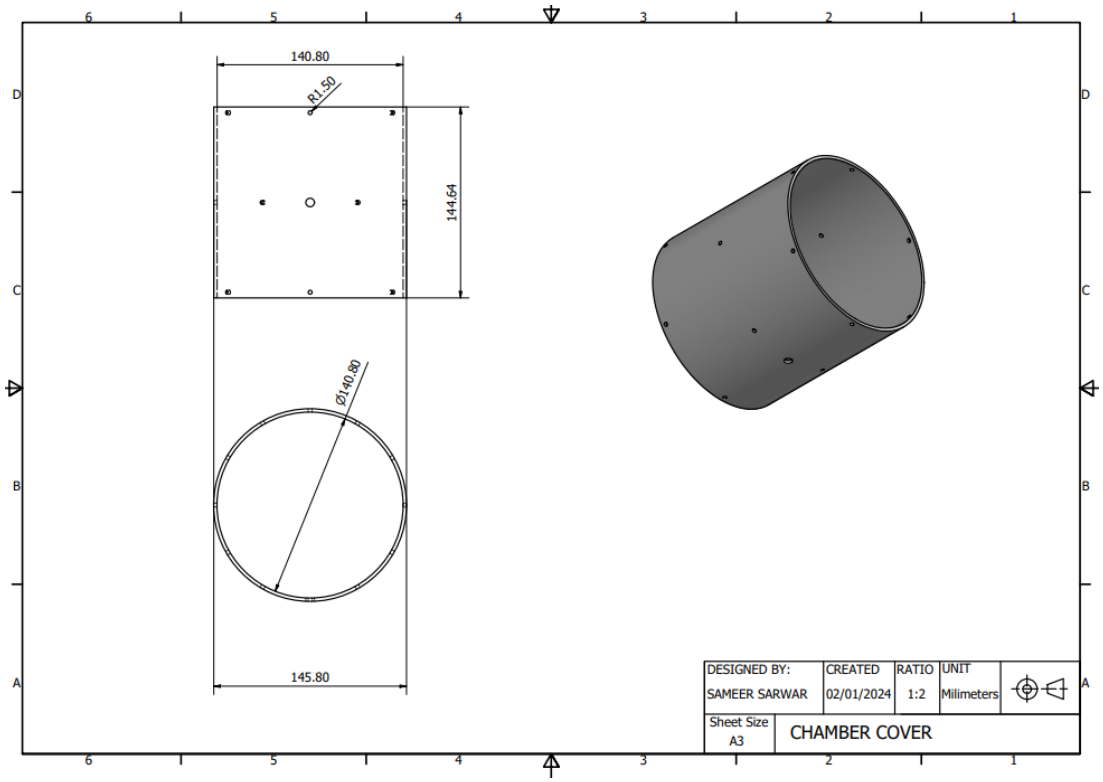

Chamber Cover

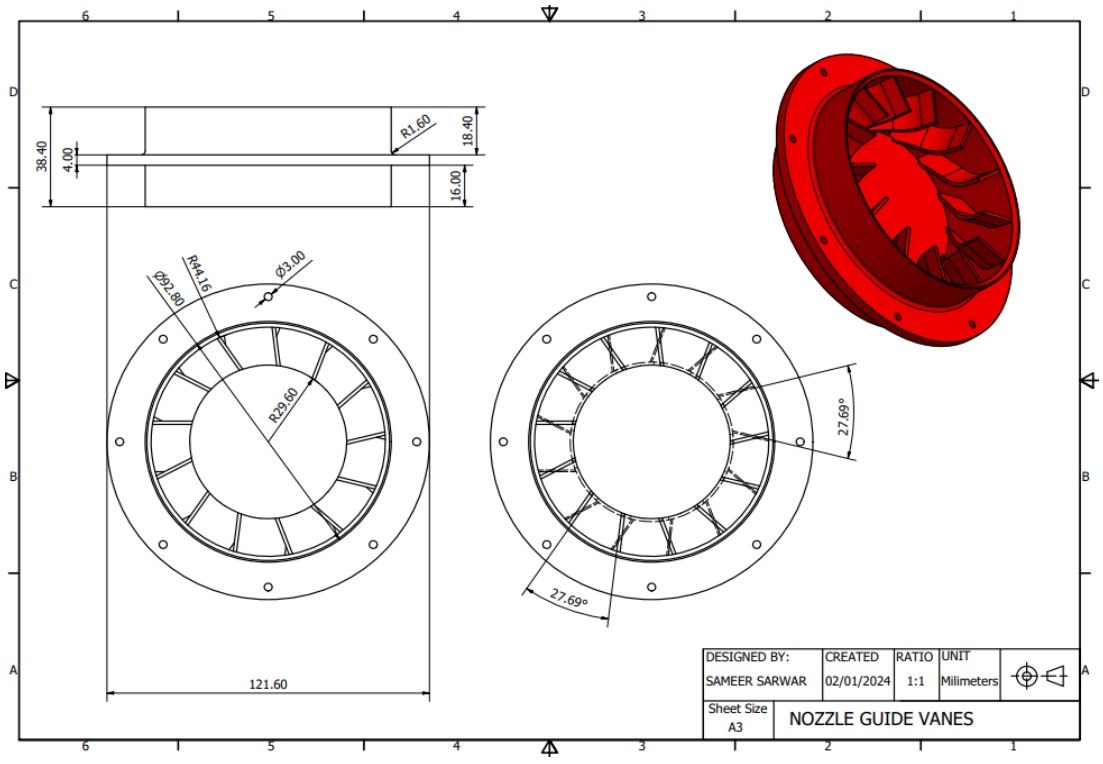

Nozzle Guide Vanes

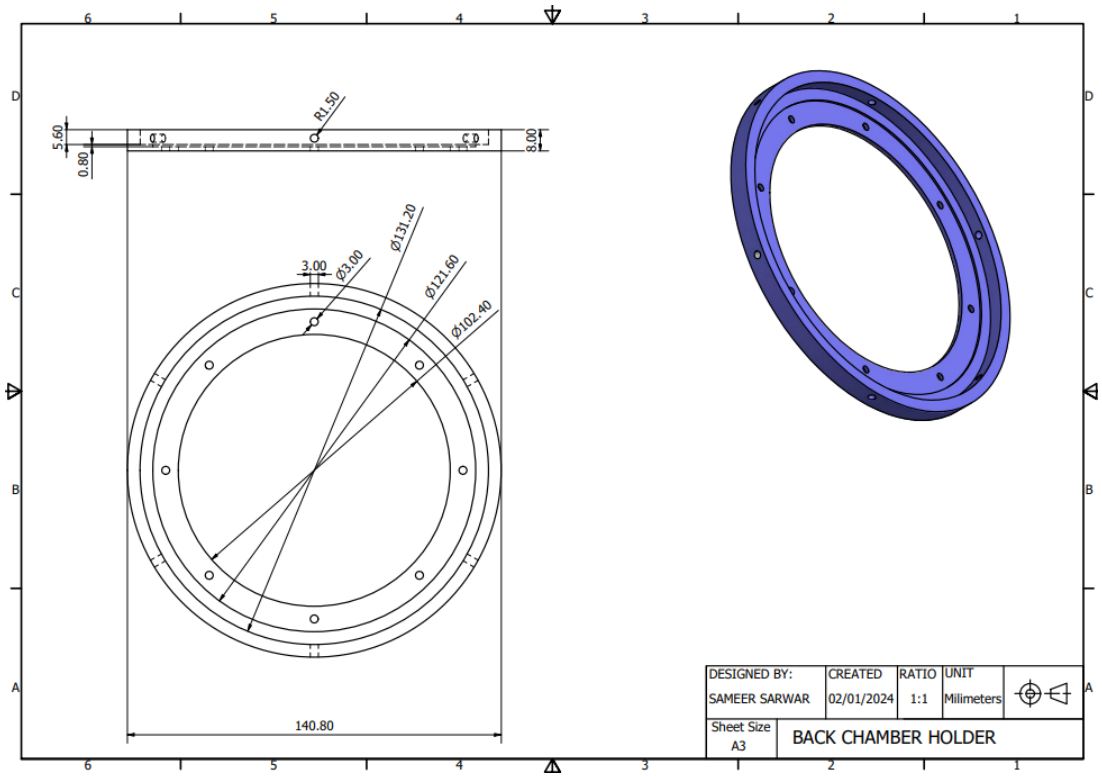

Rear Chamber Holder

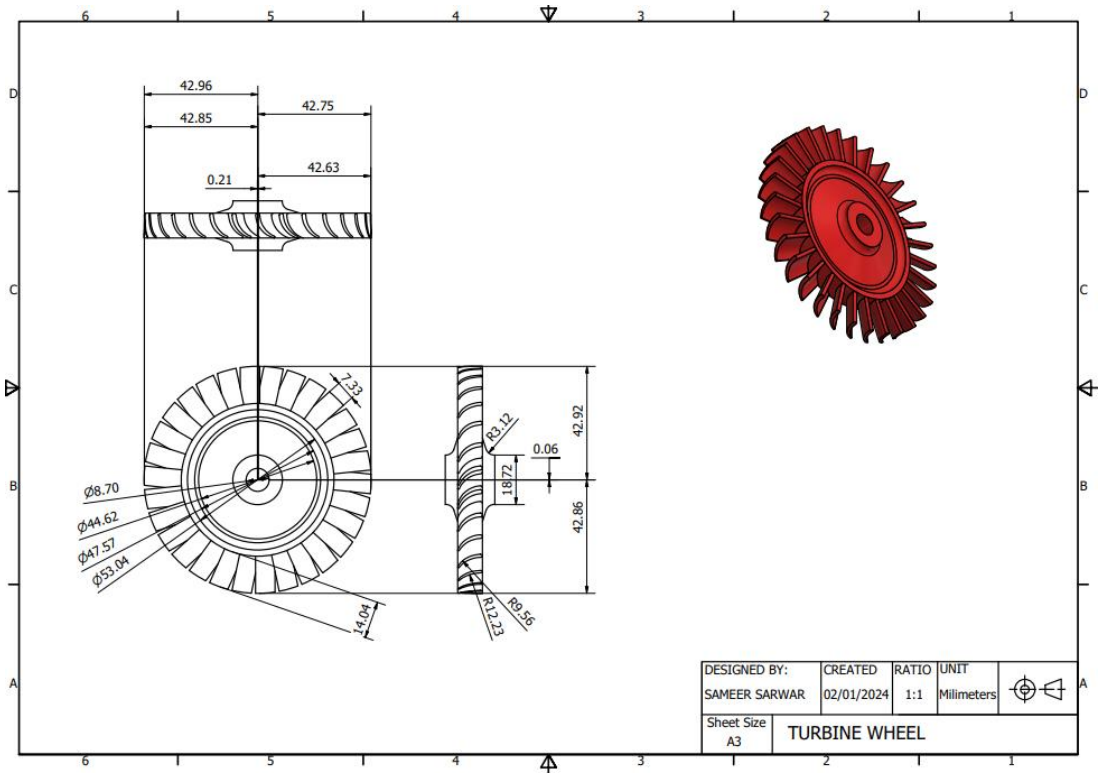

Turbine Wheel

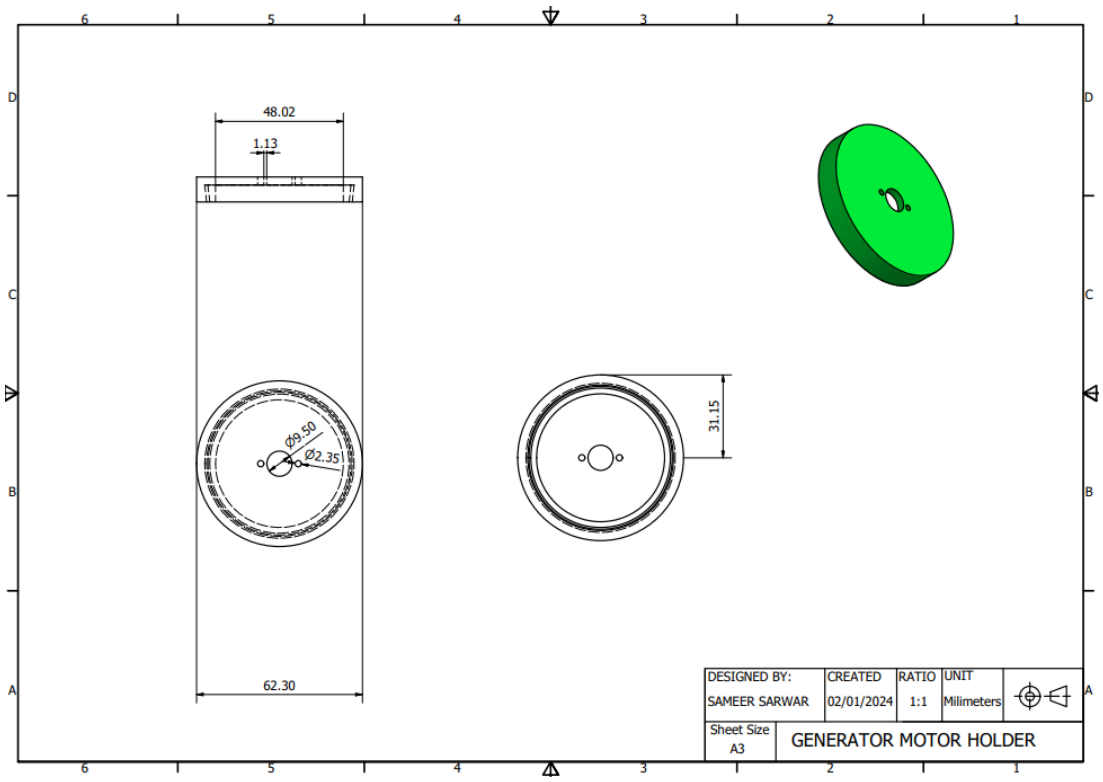

Generator Motor Holder

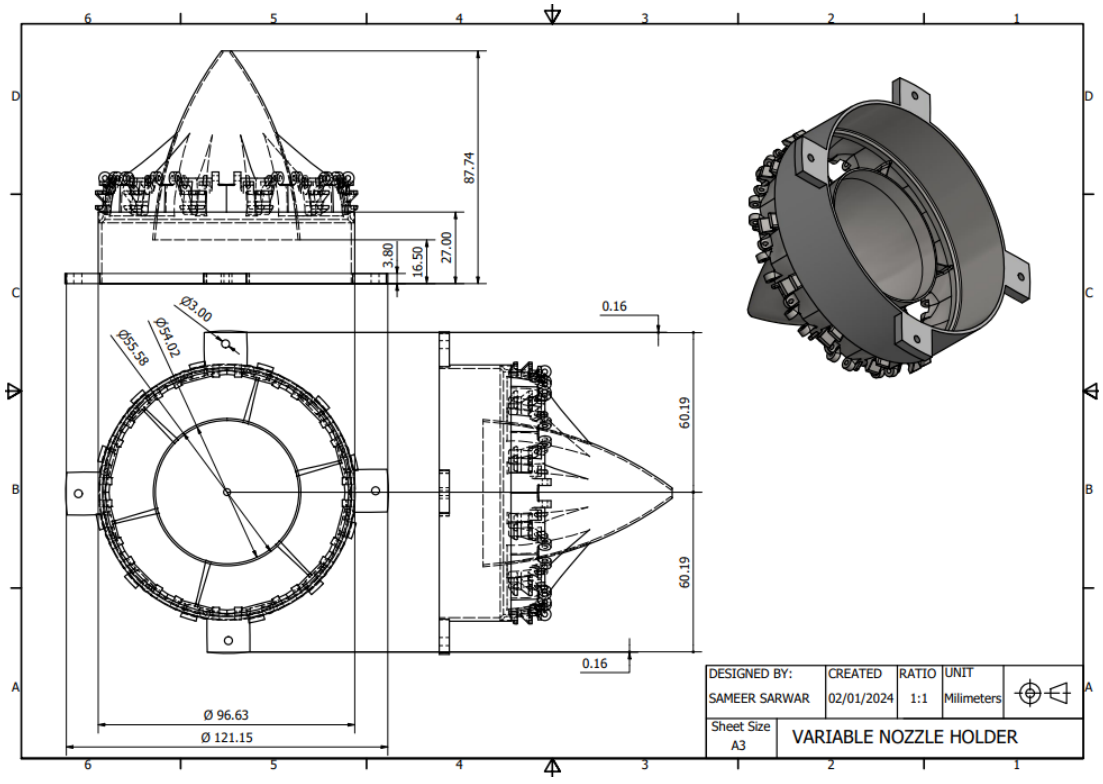

Variable Nozzle Holder

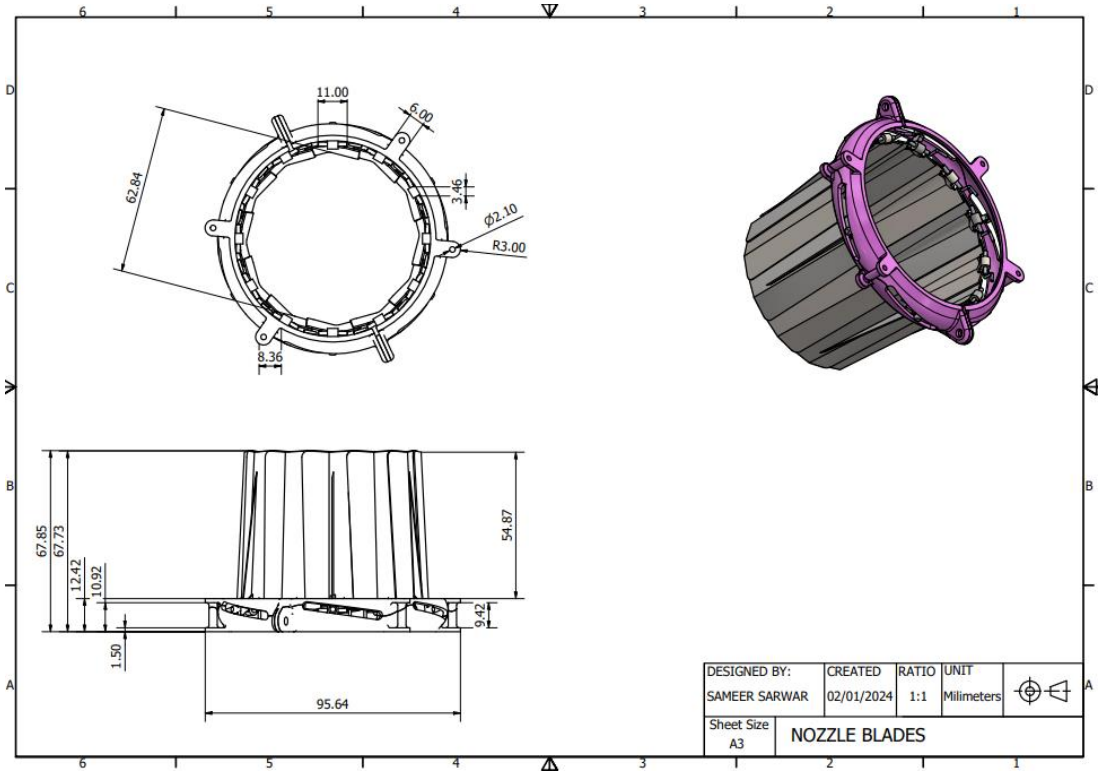

Nozzle Blade Assembly

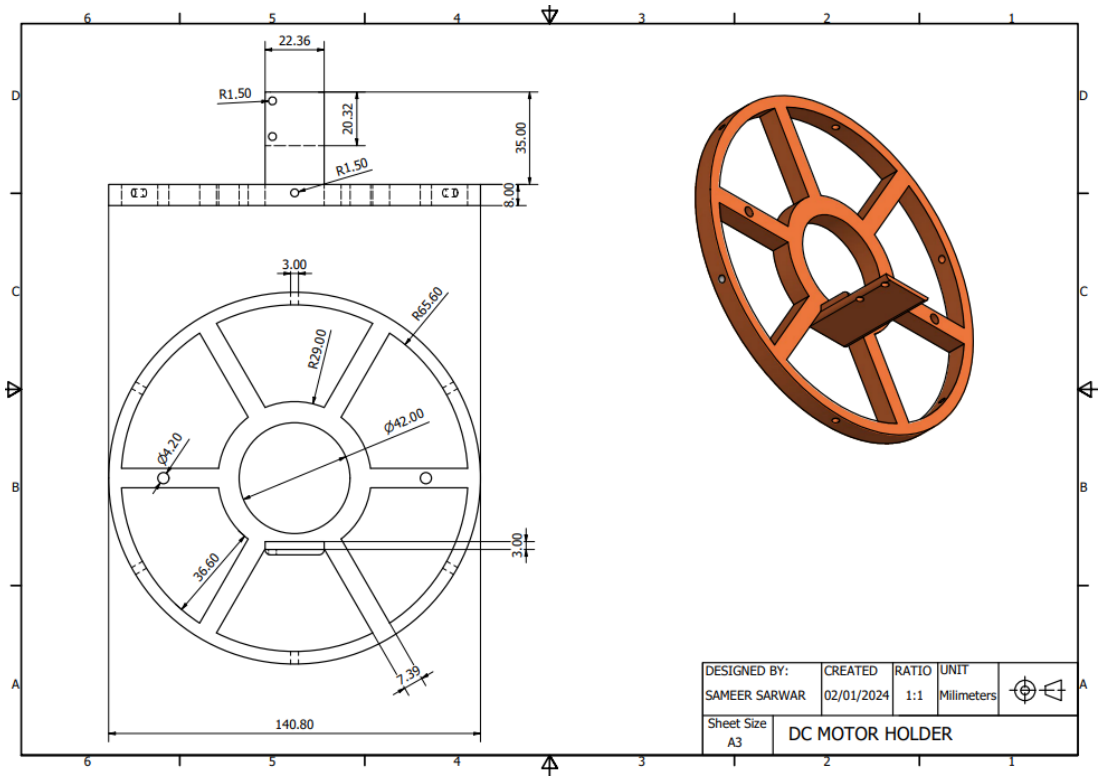

DC Motor Holder